AFRL-RI-RS-TR-2012-167

MULTI-SENSOR ELINT DEVELOPMENT (MSED)

STATE UNIVERSITY OF NEW YORK AT BINGHAMTON

JUNE 2012

FINAL TECHNICAL REPORT

APPROVED FOR PUBLIC RELEASE; DISTRIBUTION UNLIMITED.

STINFO COPY

AIR FORCE RESEARCH LABORATORY
INFORMATION DIRECTORATE

■ **AIR FORCE MATERIEL COMMAND** ■ **UNITED STATES AIR FORCE** ■ **ROME, NY 13441**

NOTICE AND SIGNATURE PAGE

Using Government drawings, specifications, or other data included in this document for any purpose other than Government procurement does not in any way obligate the U.S. Government. The fact that the Government formulated or supplied the drawings, specifications, or other data does not license the holder or any other person or corporation; or convey any rights or permission to manufacture, use, or sell any patented invention that may relate to them.

This report is the result of contracted fundamental research deemed exempt from public affairs security and policy review in accordance with SAF/AQR memorandum dated 10 Dec 08 and AFRL/CA policy clarification memorandum dated 16 Jan 09. This report is available to the general public, including foreign nationals. Copies may be obtained from the Defense Technical Information Center (DTIC) (http://www.dtic.mil).

AFRL-RI-RS-TR-2012-167 HAS BEEN REVIEWED AND IS APPROVED FOR PUBLICATION IN ACCORDANCE WITH ASSIGNED DISTRIBUTION STATEMENT.

FOR THE DIRECTOR:

/s/
PETER ZULCH
Work Unit Manager

/s/
WARREN H. DEBANY, JR.
Technical Advisor, Information Exploitation and Operations Division
Information Directorate

This report is published in the interest of scientific and technical information exchange, and its publication does not constitute the Government's approval or disapproval of its ideas or findings.

REPORT DOCUMENTATION PAGE

Form Approved
OMB No. 0704-0188

PLEASE DO NOT RETURN YOUR FORM TO THE ABOVE ADDRESS.

1. REPORT DATE *(DD-MM-YYYY)*	2. REPORT TYPE	3. DATES COVERED *(From - To)*
JUNE 2012	Final Technical Report	JAN 2009 – JAN 2012

4. TITLE AND SUBTITLE

Multi-Sensor ELINT Development (MSED)

5a. CONTRACT NUMBER
FA8750-09-2-0068

5b. GRANT NUMBER
N/A

5c. PROGRAM ELEMENT NUMBER
62788F

6. AUTHOR(S)

Mark Fowler

5d. PROJECT NUMBER
1078

5e. TASK NUMBER
BA

5f. WORK UNIT NUMBER
9D

7. PERFORMING ORGANIZATION NAME(S) AND ADDRESS(ES)

State University of NY at Binghamton
Dept. of Electrical and Computer Engineering
PO Box 6000
Binghamton, NY 13902

8. PERFORMING ORGANIZATION REPORT NUMBER

9. SPONSORING/MONITORING AGENCY NAME(S) AND ADDRESS(ES)

Air Force Research Laboratory/Information Directorate
Rome Research Site/RIGC
525 Brooks Road
Rome NY 13441

10. SPONSOR/MONITOR'S ACRONYM(S)
AFRL/RI

11. SPONSORING/MONITORING AGENCY REPORT NUMBER
AFRL-RI-RS-TR-2012-167

12. DISTRIBUTION AVAILABILITY STATEMENT

Approved for Public Release; Distribution Unlimited. This report is the result of contracted fundamental research deemed exempt from public affairs security and policy review in accordance with SAF/AQR memorandum dated 10 Dec 08 and AFRL/CA policy clarification memorandum dated 16 Jan 09.

13. SUPPLEMENTARY NOTES

14. ABSTRACT

New geolocation methods are needed that will allow accurate location of LPI emitters despite low signal-to-noise ratio (SNR) and multipath propagation. To address this recent work has provided a single-stage localization method called Direct Position Determination (DPD). However, all its computation is concentrated at one computing node. We developed several methods to remedy this problem.

To provide even better performance in these challenging real-world scenarios we developed a one-stage TDOA/FDOA localization method based on spatial sparsity of emitters. The proposed sparsity-based method has better performance (especially in multi-path and multi-emitter cases) compared to direct position determination (DPD) and two-stage Classic localization methods.

15. SUBJECT TERMS

Radio Frequency Geo-location, SIGINT, Detection and Geo-location

16. SECURITY CLASSIFICATION OF:			17. LIMITATION OF ABSTRACT	18. NUMBER OF PAGES	19a. NAME OF RESPONSIBLE PERSON
a. REPORT	b. ABSTRACT	c. THIS PAGE			PETER ZULCH
U	U	U	UU	39	19b. TELEPHONE NUMBER (*Include area code*) N/A

Standard Form 298 (Rev. 8-98)
Prescribed by ANSI Std. Z39

TABLE OF CONTENTS

List of Figures

1.0 SUMMARY

The global advancement and proliferation of high performance radio frequency (RF) commercial-off-the-shelf (COTS) technologies has created significant challenges to electronics intelligence (ELINT) and Communication Intelligence (COMINT) operations. As a consequence, entirely new methods of signal exploitation must be developed and fielded to meet these challenges. This work focused on multi-sensor algorithmic approaches for the geo-location of LPI signals in environments with significant multipath and co-channel signals. While many classical techniques exist, new methods are needed that will allow accurate location of LPI emitters despite low signal-to-noise ratio (SNR) and multipath propagation. Geo-location systems based on time-difference-of-arrival (TDOA) and frequency-difference-of-arrival (FDOA) estimate the TDOA/FDOA between a pair of signals by computing their cross-ambiguity function (CAF) and finding the location of the peak on the surface of this 2-D function. However, when multipath signals are received at each platform they give rise to spurious peaks on the CAF that can perturb the location of the true peak, especially if the spurious peaks are located close to the true peak.

This classical approach uses two stages to estimate the signal position. In the first stage, TDOA/FDOA are estimated by several pairs of sensors and then used in the second stage to locate the emitter. However, this two-stage method is known to perform poorly in low SNR cases and especially in the presence of multipath and multiple co-channel emitters. To address the drawbacks of the two-stage method, recent work has proposed a single-stage method based on TDOA/FDOA; that method is called Direct Position Determination (DPD). However, that improvement comes at a cost of significantly more computational complexity, and unfortunately that complexity is all concentrated at one computing node, unlike in the classical method where the computations are distributed evenly among the sensors. As originally proposed, the single-stage method transmits all data to a single sensor, which then forms a myriad of matrices (one for each possible emitter location grid point) and computes the maximum eigenvalue of each one. The largest of these maximum eigenvalue then indicates the emitter location.

We developed several methods to ease the application of the new single-stage method. In particular, we show how to reduce the load of data computation and data transmission using distributed data computation and processing, applying data compression methods, exploiting the CAF properties, taking advantage of CAF relationships in the sensor network and exploiting some kind of beneficial approximations. We proposed three alternative processing schemes. The *Approximated DPD* method exploits the simplicity of Gershgorin's theorem to approximately compute the maximum eigenvalue without the high cost of exactly computing it. This enables each sensor to locally make its best estimate of the location based on that data it has. These locally-generated estimates are then transmitted to a central location where a final decision is made. In *Decentralized DPD* method, we applied the distributed computation idea to divide the mathematical calculation load among all sensors of the network. In this method, we don't use any other approximation more than data compression and the quality of this method is the same as the Original DPD for reasonable bit rates. Finally, in *Semi-Optimal Decentralized DPD*, we used the same idea of Decentralized DPD in addition to exploiting the relationship between different CAFs to eliminate the data redundancy and this idea leads to a large data transmission reduction. All of the proposed methods allows DPD to be implemented in a

decentralized manner where no single sensor is required to do an unfair share of the computations, yet the performance improvement of DPD is not sacrificed.

Although the DPD method provides improved location performance at low SNR it is not as robust as desired in the presence of multipath and/or multiple co-channel emitters. To provide better performance in these challenging real-world scenarios we developed a one-stage TDOA/FDOA localization method based on spatial sparsity of emitters. In this method, we imagine assigning a non-zero number to each one of the grid points containing an emitter and zero to the rest of the grid points. Thus, the vector formed from these numbers will be a sparse unknown vector that we aim to estimate. Since each element of this vector corresponds to one grid point in the (x,y) plane, we can estimate the location of emitters by extracting the position of non-zero elements of the sparsest vector that satisfies the TDOA/FDOA relationship between transmitted signals and received signals. The proposed sparsity-based method has better performance (especially in multi-path and multi-emitter cases) compared to direct position determination (DPD) and two-stage Classic localization methods.

2.0 INTRODUCTION

The global advancement and proliferation of high performance radio frequency (RF) commercial-off-the-shelf (COTS) technologies has created significant challenges to electronics intelligence (ELINT) operations. Typically ELINT refers to RADAR signals, however the same issues have also faced Communication Intelligence (COMINT). For example, technology advances such as digital arbitrary waveform generators (DAWGs), solid state transmitters, active electronically scanned arrays (AESAs), high speed analog-to-digital converters (ADCs), and spread spectrum low-probability-of-intercept (LPI) waveforms, have given rise to a new class of signals that are extremely difficult to detect, de-interleave and characterize. While ELINT receivers have increased their operating bandwidths, that alone is insufficient to guarantee successful intercept as this is a necessary but not sufficient condition. As a consequence, entirely new methods of signal exploitation must be developed and fielded to meet these challenges.

This work focused on multi-sensor algorithmic approaches for the geo-location of LPI signals in environments with significant multipath and co-channel signals. While many classical techniques exist, new methods are needed that will allow accurate location of LPI emitters despite low signal-to-noise ratio (SNR) and multipath propagation. Geo-location systems based on TDOA/FDOA estimate the TDOA/FDOA between a pair of signals by computing their cross-ambiguity function (CAF) and finding the location of the peak on the surface of this 2-D function. However, when multipath signals are received at each platform they give rise to spurious peaks on the CAF that can perturb the location of the true peak, especially if the spurious peaks are located close to the true peak.

3.0 METHODS, ASSUMPTIONS, AND PROCEDURES

One of the most accurate and common methods for passive radio signal geolocation is based on TDOA/FDOA estimation. The classical approach to this method uses two stages to estimate the signal position. In the first stage, frequency-difference-of-arrival (FDOA) and time-difference-of-arrival (TDOA) are estimated from the cross-correlation of signals received by

several pairs of sensors [1]; this is done by computing the cross ambiguity function (CAF) [2] and finding the peak of its magnitude surface [1], [2]. In [4] and [5], a Fisher Information based data compression method has been suggested to reduce the amount of data transmission and improve the communication performance between each pair of sensors. In the second stage of the classic method, the TDOA/FDOA estimates are used in statistical processing to locate the emitter [3].

Suppose that the lowpass equivalent (LPE) model of the received signal is:

$$\hat{s}_r(t) = \alpha e^{j\omega_d t}\hat{s}(t-\tau_d) + v(t), \tag{1}$$

where $\hat{s}(t)$ is the LPE of the transmitted signal, w_d is the Doppler, τ_d is the delay for the received signal, α is a complex number and $v(t)$ is the LPE of the noise [11]. Now, suppose that two sensors R1 and R2 receive the LPE signals $\hat{s}_{r1}(t)$ and $\hat{s}_{r2}(t)$, respectively. Stein [1] showed that the maximum likelihood (ML) estimate for TDOA and FDOA can be obtained by finding the peak of the magnitude of the CAF:

$$CAF_{12}(\tau,\omega) = \int_{-\infty}^{+\infty} \hat{s}_{r1}(t)\hat{s}_{r2}^{*}(t-\tau)e^{i\omega t}dt, \tag{2}$$

which measures the correlation between $\hat{s}_{r1}(t)$ and a Doppler-shifted by ω and delayed by τ version of $\hat{s}_{r2}(t)$. The accuracy of the first stage is governed by the Cramer-Rao lower bounds (CRLB) for TDOA and FDOA. Stein [2], Wax [20], Fowler and Hu [21] and Yeredor and Angel [22] derived formulas for the CRLB on TDOA and FDOA. Yereder [22] have derived the CRLB for general unknown deterministic signals and the simulation results show that his approach obtains more accurate results compared to other CRLB formulas.

Recently, some new methods based on TDOA/FDOA emitter location have been proposed that estimate the emitter location in one stage without extracting the TDOA/FDOA in a separate stage. The goal of these methods is to improve the overall accuracy of the emitter location estimate especially in low SNR cases. Weiss and Amar [7], [8], [9] showed that the two-stage methods are not necessarily optimal because in the first stage of these methods, the TDOA and FDOA estimates are obtained by ignoring the fact that all measurements should be consistent with a single emitter location. In other words, we can say that each TDOA/FDOA estimation is optimal in the first stage. Also in the second stage, the location estimation is also optimal based on TDOA/FDOA's obtained from the first stage. But, it does not necessarily mean that the whole two-stage method is optimal.

In related work, Kay and Vankayalapati [19] developed the generalized likelihood ratio (GLR) detector based on the received signals from all sensors and the DPD location result appears as the ML estimate used in the GLR. This shows another advantage of DPD over the classical two-stage method: the classical method can't make use of the data from a CAF whose peak is undetectable due to low SNR – yet the DPD method can.

However, there are some issues that need to be addressed. Namely, the implementation of the DPD method has many challenges, such as how to distribute the computation across the participating sensors and how to efficiently communicate the necessary data between the sensors. Furthermore, the performance of the DPD method in the presence of multipath and multiple co-channel emitters was previously unknown. This report addresses the distributed

computation/communication issues of DPD and also demonstrates that DPD performance can suffer in the presence of multipath and multiple co-channel emitters. To address these shortcomings we have extended the general single-stage idea to be able exploit the sparsity of emitters in the geometrical region.

4.0 RESULTS AND DISCUSSION

4.1 Communication and Distributed Computation for Single-Stage TDOA/FDOA Location

In the DPD method, we need all the received signals together at a single point to start the location estimation processing. Consequently, all sensors have to transmit their received signals to a common site, which usually is one of the sensors so we will refer to this as the common sensor. The common sensor then uses the received signals to form a series of matrices (one for each point on an x-y location grid) and computes the maximum eigenvalue of each of these matrices; the location estimate is the grid point that produced the largest of these maximum eigenvalues.

As mentioned above, the one-stage DPD method achieves more accurate results compared to classic two-stage methods. However, in the published papers, the authors did not address the issues of computation and data transmission for DPD and there are some difficulties that may limit DPD applications in practice. The first problem is the large amount of computations that are to be done by only the common sensor. As mentioned above, in DPD method we need all received signals together to start the estimation process. Thus, all sensors should send their received signals to one common sensor to start the estimation process. The common sensor will do all mathematical computations having all received signals. This leads to a large computational load on only one point in the network and no computational load on other members of the sensor network, which requires any one sensor in the system to be computationally capable of doing the complete set of computations needed to locate an emitter. In scenarios where the amount of computational capabilities any one sensor possesses is limited this centralized approach is not desirable.

The second problem is the large amount data transmission to one single point. In other words, large bandwidth data links are required to transfer all received signals to the common sensor and it leads to have a bottle-neck at the common sensor channel.

The third problem is the high dependence of the whole network on the common sensor. In this scenario, if we lose the common sensor during computations, we will lose everything. In other words, it is not desirable to rely on only one point in the sensor network for computations and data collection, because if we lose that sensor for any reason, then we will lose all intermediate and final results.

In this paper, we develop some methods to increase the flexibility and feasibility and improve the performance of one-stage geolocation methods. We use distributed data compression to reduce the amount of data transmission in suggested methods and also we use distributed computations in the sensor network to reduce the mathematical computational load on the common sensor. Comparisons will be made to determine the advantages and disadvantages of each method in terms of estimation accuracy, computation load, transmission load and reliability.

4.1.1 Background

In this section we provide some more details about the DPD single-stage localization method and its formulation [9]. Suppose that there are L moving sensors in a sensor network receiving the transmitted signal in one short snapshot. The complex signal observed by the l^{th} sensor is

$$\hat{s}_{rl}(t) = \alpha_l s(t-\tau_l) e^{j2\pi f_l t} + w_l(t)$$

where $s(t)$ is the transmitted signal, α_l is an unknown complex path attenuation, , f_l is the Doppler shift, τ_l is the signal delay and $w_l(t)$ is a white, zero mean, complex Gaussian. Assume that each sensor collects N time samples sampled with sampling frequency $F_s = 1/T_s$ .Then, we have

$$\hat{\boldsymbol{s}}_{\boldsymbol{rl}} = \alpha_l \boldsymbol{W}_l \boldsymbol{D}_l \hat{\boldsymbol{s}} + \boldsymbol{w}_l$$

$$\boldsymbol{W}_l = diag\{e^{j2\pi f_l t_1}, \quad e^{j2\pi f_l t_2}, \quad \ldots \quad , \quad e^{j2\pi f_l t_N}\}$$

$$\hat{\boldsymbol{s}}_{\boldsymbol{rl}} = [\hat{s}_{rl}(t_1), \quad \hat{s}_{rl}(t_2), \quad \ldots \quad , \quad \hat{s}_{rl}(t_N)]^T$$

$$\boldsymbol{w}_l = [w_l(t_1), \quad w_l(t_2), \quad \ldots \quad , \quad w_l(t_N)]^T$$

where $\hat{\boldsymbol{s}}_{\boldsymbol{rl}}$ is N samples of the received signal at l^{th} sensor, $\hat{\boldsymbol{s}}$ is N samples of the transmitted signal, f_l is the Doppler shift and $\boldsymbol{D_l}$ is the time sample shift operator by $n_l = (\tau_l / T_s)$ samples. We can write $\boldsymbol{D}_l = \boldsymbol{D}^{n_l}$ where $\boldsymbol{D}$ is an $N \times N$ permutation matrix defined as $[\boldsymbol{D}]_{ij} = 1$ if $i = j+1$, $[\boldsymbol{D}]_{0,N-1} = 1$ and $[\boldsymbol{D}]_{ij} = 0$ otherwise.

According to [9] and [19], the estimated transmitter's position in TDOA/FDOA-based one-stage method is found as follows. Let $\{\mathbf{p}_i\}_{i=1}^{G}$ be grid points of possible emitter locations. For each grid point form the matrix

$$\boldsymbol{V}_{\boldsymbol{p}_i} = \left[\boldsymbol{D}_1^{\,H} \boldsymbol{W}_1^{\,H} \hat{\boldsymbol{s}}_{r1}, \quad \boldsymbol{D}_2^{\,H} \boldsymbol{W}_2^{\,H} \hat{\boldsymbol{s}}_{r2}, \quad \ldots, \quad \boldsymbol{D}_L^{\,H} \boldsymbol{W}_L^{\,H} \hat{\boldsymbol{s}}_{rL} \right],$$

where the dalay and Doppler operators correspond to the path between the grid point and the respective sensors [9]. For each grid point, then form the $L \times L$ matrix $\boldsymbol{Q}_{\boldsymbol{p}_i} = \boldsymbol{V}_{\boldsymbol{p}_i}^{H} \boldsymbol{V}_{\boldsymbol{p}_i}$ and find its largest eigenvalue. The location estimate is the grid point that maximizes the largest eigenvalue, that is

$$\hat{\boldsymbol{p}} = \arg\max_{\boldsymbol{p}_i} \{\lambda_{\max}(\boldsymbol{Q}_{\boldsymbol{p}_i})\}. \tag{3}$$

Since all of this process should be done for each one of the grid points, it is clear that a large amount of computation must be done to find the location and all of it is done at the common sensor.

It is interesting to mention that in TDOA/FDOA based one-stage method, the (*i*,*j*)th element of the matrix $\boldsymbol{Q}$ is the value of CAF between the signals received by sensors i and sensor j [9], [19] and that is why in [19], this matrix is called the Cross Ambiguity Matrix (CAM):

$$[\boldsymbol{Q}]_{ij} = [\boldsymbol{V}^H \boldsymbol{V}]_{ij} = \hat{\boldsymbol{s}}_{ri}^{\ H} \boldsymbol{W}_i \boldsymbol{D}_i \boldsymbol{D}_j^{\ H} \boldsymbol{W}_j^{\ H} \hat{\boldsymbol{s}}_{rj} = [\boldsymbol{CAF}_{ij}]_{(\tau,\omega)}, \tag{4}$$

where τ and ω are the corresponding TDOA and FDOA between sensors *i* and *j* and emitter located at a specific emitter position. Note that the diagonal elements in CAM are the Auto Ambiguity Function of the received signals at TDOA = 0 and FDOA = 0 which is equal to the energy of the received signals.

In the following, we develop some methods to increase the flexibility and feasibility and improve the performance of one-stage geolocation method.

4.1.2 Approximated DPD

As mentioned above, in one-stage geolocation method, we need all the received signals together to start the location estimation process. To achieve that, all sensors need to transmit their received signals to a common point. The common site performs a huge mathematical computation on the raw received signals to form a series of matrices used in location estimation [7],[8], [9]. In this section we develop a method to distribute and reduce the amount computation based on the eigenvalue approximation.

Definition (Gershgorin's disc)[29]: Assume that $\boldsymbol{A}$ is an $n \times n$ complex valued matrix with entries a_{ij} and $P_i = \sum_{j \neq i} |a_{ij}|$ is the summation of the absolute values of all non-diagonal elements of the i^{th} row. Then, the set $D_i = \{ z \in C : |z - a_{ii}| \leq P_i \}$ is called the i^{th} Gershgorin's disc of $\boldsymbol{A}$, where *C* is the set of complex numbers. This disc contains the interior and boundary points of a circle with radius of P_i and centered at a_{ii} in complex plane.

Theorem 1 (Gershgorin's Theorem) [29]: Every eigenvalue of matrix $\boldsymbol{A} = [a_{ij}] \in C^{n \times n}$ lies within at least one of the Gershgorin's discs. In other words, every eigenvalue λ of matrix $\boldsymbol{A}$ satisfies:

$$\begin{aligned} &\forall \lambda, \exists i \quad |\lambda - a_{ii}| \leq P_i, \\ &P_i = \sum_{j \neq i} |a_{ij}|. \end{aligned} \tag{5}$$

Theorem 2 [29]: Assume that $\boldsymbol{A}$ is an $n \times n$ complex valued matrix with entries a_{ij}, $R_i = \sum_j |a_{ij}|$ is the summation of the absolute values of all elements in the i^{th} row and $T_j = \sum_i |a_{ij}|$ is the summation of the absolute values of all elements in the j^{th} column. Let $R = \max_i R_i$ and $T = \max_j T_j$. Then, the absolute value of each eigenvalue λ of matrix $\boldsymbol{A}$ satisfies:

$$\forall \lambda, \quad |\lambda| \leq \min(R, T). \tag{6}$$

As mentioned above, in TDOA/FDOA based one-stage method, the $(i,j)^{th}$ element of the CAM or $\boldsymbol{Q}$ in (3) is the value of Cross Ambiguity Function between the signals received by sensors i and sensor j ([9],[19]) and we name it by CAF_{ij}. The emitter location is estimated by computing the maximum eigenvalues of the CAM (or Q) in each grid point. Since the CAM is Hermitian and positive definite, the eigenvalues of CAM are real and positive. Moreover, since CAM is a Hermitian matrix, we have, $R = T$ in Theorem2 and consequently, $\min(R,T) = R$. Thus, for the CAM, the inequality in (6) can be replaced by:

$$\begin{aligned} &\forall \lambda, \quad \lambda \le \max_i (CAF_i) \\ &CAF_i = \sum_j \left| CAF_{ij} \right| \\ &\hat{\lambda}_{\max} = \max_i (CAF_i) \end{aligned} \tag{7}$$

where $\hat{\lambda}_{\max}$ is the upper bound on eigenvalues of the CAM.

Suppose that we have L receiving sensors and each one of them broadcasts its received signal to all other sensors in the sensor network. Then, each sensor i is able to compute all CAF_{ij} for $j=1...\ L$ and consequently, it is able to compute $CAF_i = \sum_{j=1}^{L} \left| CAF_{ij} \right|$. Now, if we approximate the largest eigenvalue of CAM by the upper bound on the eigenvalues ($\lambda_{\max} \approx \hat{\lambda}_{\max}$), then the location estimation will be determined by the point having the largest $\hat{\lambda}_{\max}$.

Here is the scenario:

1- Each sensor broadcasts its received signal in the sensor network.
2- Each sensor i computes CAF_{ij}'s in TDOA/FDOA plane and then maps them from TDOA-FDOA plane to X-Y (emitter position) plane. The mapping will be done very easily knowing the position and velocity of the sensors and also the grid point position.
3- Each sensor i computes $CAF_i = \sum_{j=1}^{L} \left| CAF_{ij} \right|$ by adding up the CAF_{ij}'s and then finds the peak of CAF_i (named $CAF_{i,peak}$) and its location $(x_{i,peak}, y_{i,peak})$ and then transfers the three numbers $x_{i,peak}, y_{i,peak}$ and $CAF_{i,peak}$ to a common sensor (or to all other sensors since there are just three numbers and there is no communication load to transfer them). Note that this step is motivated by Gershgorin's Theorem.
4- According to (3) and (7), the emitter location estimated is taken as the $(x_{i,peak}, y_{i,peak})$ corresponding to the largest $CAF_{i,peak}$ over all i.

Note that in the original DPD method, we need to re-compute and form the matrix CAM (or $\boldsymbol{Q}$) *for each grid point* and find the largest eigenvalue of that matrix each time, which leads to a huge amount of computation especially when the number of receiving sensors gets larger. Moreover, all of these computations would be done at one single point. But, the method outlined

above does not need to form the matrix CAM (or $\boldsymbol{Q}$) at all nor does it need to do computationally expensive computations of the largest eigenvalue each time. Thus, in the new method, not only has the costly eigenvalue computation been removed, but also the process is distributed among all receiving sensors. When implementing DPD in a scenario where each sensor has limited computational abilities it is desirable to minimize the amount of computation done by each sensor rather than minimize the total computational complexity. To compare the computational load suppose that there are L sensors trying to estimate the emitter location in an $N \times N$ grid plane. In the original DPD method, the common sensor needs to compute the CAM for each grid point. Since CAM is a Hermitian $L \times L$ matrix formed by CAFs, the common sensor just needs to find all the entries on and above the main diagonal. This is equivalent to computing $\frac{L}{2}(L-1)$ CAFs (as non-diagonal elements) and L signal energies (as diagonal elements). Moreover, the common sensor needs to calculate the largest eigenvalue of the matrix for each grid point (N^2 times). On the other hand, in the suggested method, each sensor just needs to find $(L-1)$ CAFs and one signal energy. In addition, they don't need to form the matrix CAM and find its eigenvalues. Thus, rather than having one sensor compute $\frac{L}{2}(L-1)$ CAFs as in the original DPD, in the method propose here each sensor computes only (L – 1) CAFs; furthermore, each sensor performs a simple Gershgorin estimation rather than a complex eigenvalue computation.

It is worth saying that in the proposed method, if we lose anyone of the sensors or even if we lose a couple of them, it may reduce the accuracy of estimation because of missing some data but, the rest of the receivers can continue the estimation process with no interruption.

In the proposed method, if we ignore the maximum operator term in (7) and just take $\hat{\lambda}_{\max} = CAF_i$ for only one arbitrary sensor i , then the results will be equivalent to a method named CAF-MAP in [6] which has less quality compared to DPD and Approximated DPD. In [19], we can also see another approach named as *pair-wise maximum CAF detector* that is based on comparing the value of $\max_j \max_{\tau,\omega} \left| CAF_{ij} \right|$ with a threshold γ_{CAF} for only one arbitrary i as reference sensor (τ, ω are TDOA and FDOA). The results in [19] showed that this method also has much lower quality in detection compared to the GLRT detector based on largest eigenvalue; no results were provided in [19] on the location accuracy of the pair-wise maximum CAF method.

The simulation results for many different cases show that the eigenvalue upper bound is very close to the true largest eigenvalue. However, this approximation lowers the quality of the estimation slightly. We examined the effect of the proposed approximation on the estimation accuracy using Monte-Carlo computer simulations (with 500 runs each time). In this simulation, a set of 8 moving sensors and one stationary emitter are placed in a configuration as shown in Figure 1. There exists a cross ambiguity function for each two of the sensors. The sampling frequency is 80 kHz and the number of samples is equal to 4096. Figure 2 shows the effect of eigenvalue approximation on RMS error of emitter location estimation for X and Y dimensions.

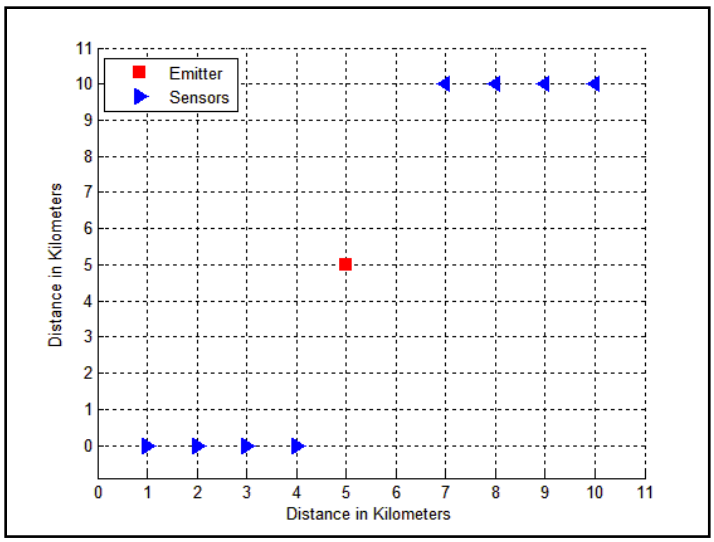

Figure 1: Placement of the sensors and the emitter position used for simulation.

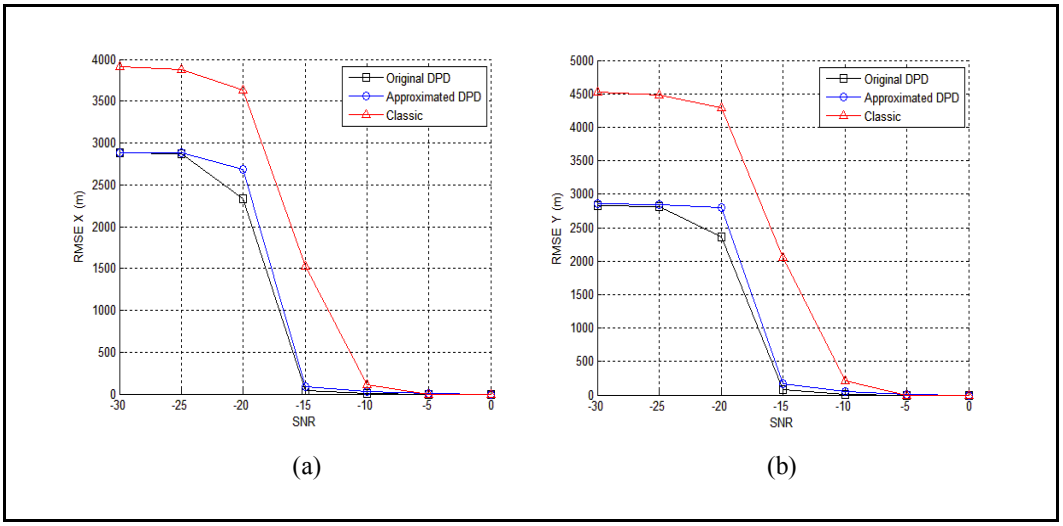

Figure 2: RMS errors for X and Y versus SNR.

In the suggested method, if we ignore the maximum operator term in (7) and just take $\hat{\lambda}_{\max} = CAF_i$ for only one arbitrary sensor i, then the results will be equivalent to a method named CAF-MAP in [6] which has less quality compared to DPD and Approximated DPD. In [19], we can also see another approach named as *pair-wise maximum CAF detector* that is based on comparing the value of $\max_j \max_{\tau,\omega} \left| CAF_{ij} \right|$ with a threshold γ_{CAF} for only one arbitrary i as reference sensor (τ, ω are TDOA and FDOA). The results in [19] showed that this method also has much less quality in detection compared to the GLRT detector based on largest eigenvalue.

4.1.3 Decentralized DPD

In this section, we develop another method to implement DPD with the goal of reducing the computation load on the center point by distributing the mathematical computations among all receivers and using data compression to reduce the amount of data transmission. In this method, we don't apply any approximation more than data compression. Thus, the accuracy of this method is as same as original DPD for high enough bit rates.

4.1.3.1 Distributed Computation

As mentioned above, in DPD method a common site performs a huge mathematical computation on the raw signals received from all other sensors to form a series of matrices used in location estimation. If each sensor or pair of sensors can do some pre-processing on its own data before transmitting to the common site, it can help to do the estimation in shorter time and with less processing load on the common site. It also helps to reduce the sensitivity of the common site's role and the dependence of the whole process to one single point in the sensor network.

As mentioned above, in TDOA/FDOA based one-stage method, the (i,j)th element of the cross ambiguity matrix (CAM in [20] or $\boldsymbol{Q}$ in [9] and (3)) at grid point $\boldsymbol{p}$ is the value of Cross Ambiguity Function (CAF) between the signals received by sensors i and sensor j at TDOA/FDOA point corresponding to the grid point $\boldsymbol{p}$. Thus, sensor i and sensor j can contribute to compute the (i,j)th element of CAM (and (j,i)th element as well since CAM is a Hermitian matrix). In the other word, each pair of sensors i and j can share their received signals together to compute the CAF_{ij} in TDOA/FDOA domain. Then the computed CAFs can be transmitted to the common site. The common site only maps the received CAFs to X-Y plane and uses them to form the CAM matrix.

Figure 3 shows a simple case with three receiving sensors. In Figure 3(a), we can see the sensors sharing their received signals. Sensor 1 sends its received signal to sensor 2, sensor 2 sends its received signal to sensor 3 and sensor 3 sends its received signal to sensor 1. Then, sensor 1, sensor 2 and sensor 3 are able to compute $\boldsymbol{CAF}_{13}$, $\boldsymbol{CAF}_{12}$, $\boldsymbol{CAF}_{23}$ respectively. The terms A_{11}, A_{22}, A_{33} are the Auto Ambiguity Function of the received signals at the origin of TDOA/FDOA plane that are equal to the energy of the received signals at each receiver. In Figure 3(b), we can see the receivers transmitting the computed CAFs and Energies to a common site (that obviously can be any one of the three sensors) to form the matrix CAM. Note that each one of the $\boldsymbol{CAF}_{13}$, $\boldsymbol{CAF}_{12}$ and $\boldsymbol{CAF}_{23}$ is a complex-valued matrix used to fill out the off-diagonal elements of the CAM and A_{11}, A_{22}, A_{33} are just three real numbers sitting on the diagonal elements of the CAM.

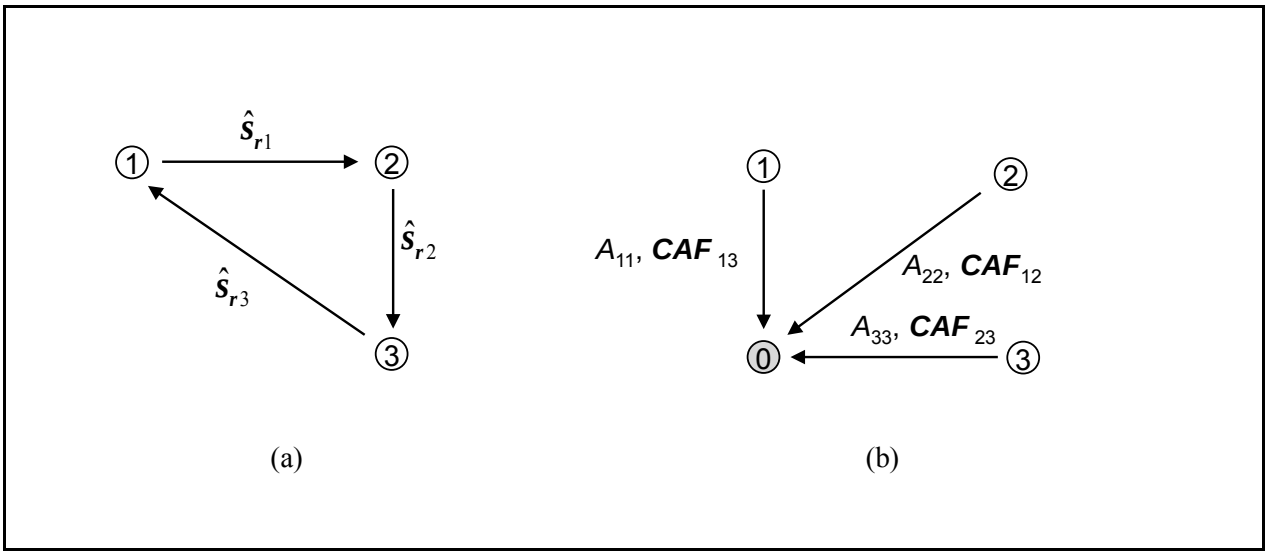

Figure 3: Decentralized DPD for three receivers.

In this method, all sensors contribute in the process of estimation and the computation load is divided among all members of the sensor network. However, this method does not help to eliminate the bottle-neck we have in data transmission since we need to transmit all CAFs to the common point. In next sub-sections, we develop some data compression ideas to compress the CAF before transmission to the common site to reduce the amount of data transmission. We exploit some of the CAF properties to eliminate the redundancy and obtain a larger compression rate.

4.1.3.2 Exploiting CAF Properties for Data Compression

To reduce the amount of data transmission and channel bandwidth in our sensor network and obtain a better performance, we apply some data compression methods in different levels of data transmission. In [4] and [5], Fowler and Chen have derived some fisher information based methods to compress the received signal in each pair of sensors. Here, we develop and apply some proper compression methods on computed CAFs before transferring it to the center site.

CAF is a two-dimensional complex valued function. Thus, we can consider the CAF to be an image (albeit a complex valued image) and apply image compression methods to it. For example, Embedded Zerotree Wavelet (EZW) [10] can be used to compress the CAF. One of the most important reasons that encourage us to use EZW method is that EZW is an embedded algorithm. It attempts to provide a sequence of bits that if truncated anywhere gives the best distortion for that rate. The EZW compression causes two kinds of distortion on the data. The first distortion refers to the effect of data quantization which can be modeled by an additive noise. The second distortion is the result of throwing away the insignificant coefficients of the wavelet transform which can be roughly modeled as passing the data through a lowpass filter. Note that a typical CAF contains a large main lobe and (usually) various small side lobes. An important aspect for compression of the CAF is that it is a relatively slowly changing function. The fast changing parts (which are equivalent to very high frequency points) come from the effect on the CAF of the additive noise of received signals. Thus, viewed as an image, it seems that the important part

to be retained is a spatially low-pass type signal that should show up in the medium and low frequency parts of the wavelet transform used in EZW. Because most of the data concentrated in medium and low frequency parts, it helps to obtain lots of zero tree roots and that is another encouraging reason to use EZW method. Because the high frequency parts of the wavelet transform will contain mostly noise and will be discarded (except at the very highest data rate, when little or no truncation is done), the EZW algorithm will also perform a denoising operation.

There are some other special properties with CAF that can be exploited to get better compression performance. One of the most important properties of CAF is the symmetry. In the Appendix we have proved that CAF is symmetric around its magnitude peak:

$$|\boldsymbol{CAF}_{ij}(-\tau+\tau_P,-\omega+\omega_P)| = |\boldsymbol{CAF}_{ij}(\tau+\tau_P,\omega+\omega_P)| \tag{8}$$

where CAF_{ij} is the cross ambiguity function between the signals received by sensor *i* and sensor *j* and (τ_p,ω_p) is the peak of CAF magnitude. This result provides a kind of symmetry of the CAF around the point (τ_p,ω_p) or the peak of CAF magnitude which can be exploited for data compression. In practice, the received signals received signals are the delayed and Doppler-shifted version of transmitted signal plus noise. This noise perturbs the CAF a little bit from the perfect symmetry. Thus, we rewrite (8) as,

$$|\boldsymbol{CAF}_{ij}(-\tau+\tau_P,-\omega+\omega_P)| = |\boldsymbol{CAF}_{ij}(\tau+\tau_P,\omega+\omega_P)|+E \tag{9}$$

where *E* can be the error from perfect symmetry which is a negligible value. Thus, using the symmetry property, it is possible to extract the entire CAF magnitude by transmission of only half of the CAF magnitude plus the small residual amount of *E*.

We examined the performance of the proposed method using Monte Carlo computer simulations. In this simulation, a set of 4 moving sensors and one stationary emitter are placed in a configuration as shown in Figure 4. There exists a cross ambiguity function for each two of the sensors that should be compressed and transmitted to a common site to do the location estimation. The signals are Binary Phase Shift Keying (BPSK) signals, the sampling frequency = 400 kHz, *SNR* = -10 dB and the number of samples is equal to 65536.Two different compression methods have been examined in this simulation. In the first method, we just applied the EZW algorithm to compress the CAF (labeled "simple compression" in the figures). In the second method, we applied the EZW algorithm to compress the CAF and we used the symmetry property to reduce the amount of transmitted data (labeled "symmetric compression" in the figures). The effect of data compression on RMS error of emitter location estimation for X and Y dimensions is illustrated in Figure 5 (a) and (b), respectively. Obviously, the RMS error will decrease by increasing the bit rate. Comparing the two curves in each plot shows that the symmetric compression method gives us more accurate results for the same bit rates.

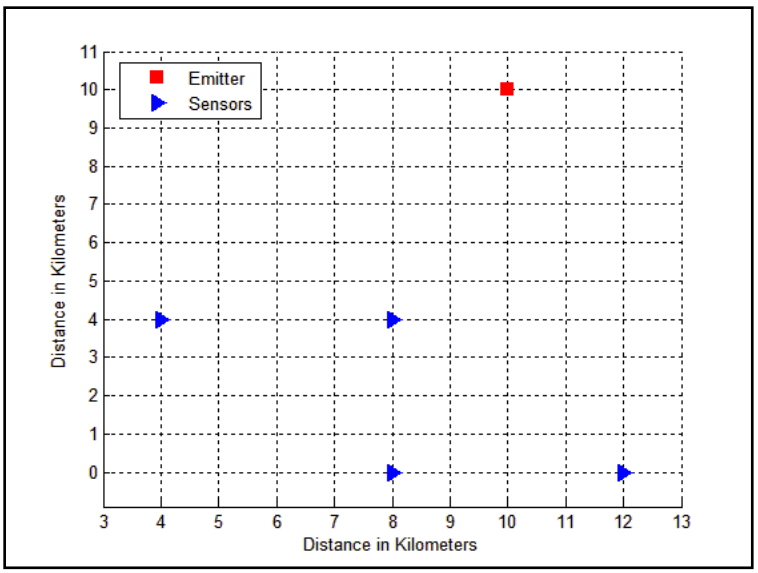

Figure 4: Placement of the sensors and the emitter position used for simulation.

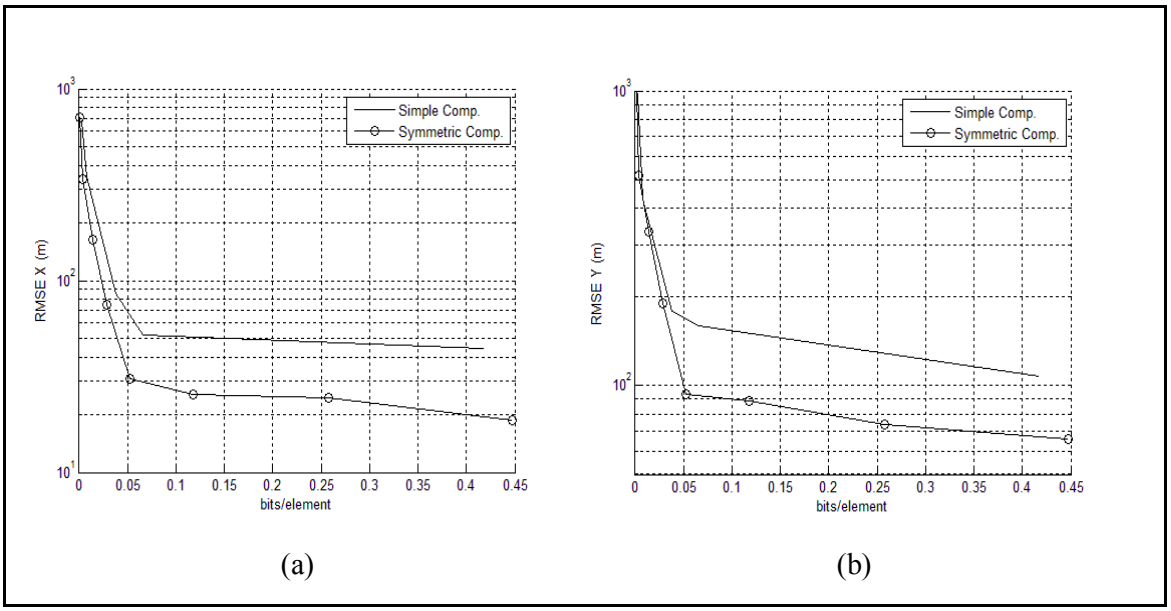

(a) (b)

Figure 5: RMS errors for X and Y versus bits/element.

4.1.3.3 SVD-based Data Compression for CAF

The singular value decomposition (SVD) is an important tool with many useful signal processing applications. For a complex valued $M \times N$ matrix $\mathbf{X}$, the SVD representation will be

$$\mathbf{X} = \mathbf{U}\boldsymbol{\Sigma}\mathbf{V}^H = \sum_{i=1}^{r} \sigma_i \mathbf{u}_i \mathbf{v}_i^H$$

where $\mathbf{U}$ is an $M \times M$ unitary matrix consisting of *M left singular vectors* as its columns, $\mathbf{V}$ is an $N \times N$ unitary matrix consisting of *N right singular vectors* as its columns and $\mathbf{\Sigma}$ is a pseudo-diagonal $M \times N$ matrix with nonnegative real *singular values* (σ_i) on the main diagonal ordered such that $\sigma_i \geq \sigma_{i+1}$, r is the number of non-zero singular values, $\mathbf{u}_i$ is the i^{th} *left singular vector* and $\mathbf{v}_i^H$ is the Hermitian transpose of the i^{th} *right singular vector*. By truncating the above summation to $k < r$ terms, we get a rank-k matrix

$$\mathbf{X}_k = \mathbf{U}_k \mathbf{\Sigma}_k \mathbf{V}_k^H = \sum_{i=1}^{k} \sigma_i \mathbf{u}_i \mathbf{v}_i^H$$

that approximates $\mathbf{X}$ better than any other rank-k matrix in the least square error sense [23], [24]. This is the main idea of SVD data compression.

The complex-valued $M \times N$ matrix $\mathbf{X}$ contains MN complex values or equivalently $2MN$ real values. However, the truncated-SVD version $\mathbf{X}_k$ uses only kM complex values to represent matrix $\mathbf{U}_k$, kN complex values for matrix $\mathbf{V}_k$, and k real values to represent the singular values. Thus, in approximation $\mathbf{X}$ by $\mathbf{X}_k$, the compression ratio is:

$$CR = \frac{2MN}{2kM + 2kN + k}.$$

For example, for a 128 ×32 matrix truncated for $k = 1$ the compression ratio is 25:1.

As mentioned in [25], the singular value decomposition of an image is conceptually similar to its Karhunen-Loeve decomposition but in a different manner. The first difference is that Karhunen-Loeve decomposition basis are determined by the covariance matrix of the random process that generates the image but, SVD is defined on the image itself. The second difference is that if both representations are truncated for the purpose of data compression, SVD is the best approximation in least square error sense, while Karhunen-Loeve is the best approximation in mean square error sense.

CAF usually contains a big main lobe and several small side lobes that if we slice each of them up at different points, we will always get a curve with a similar shape. It has been shown that for a time-frequency localization operator there are several large singular values at the beginning, followed by a sharp plunge in the values, with a final asymptotic decay to zero [26]. Since the cross Ambiguity function is considered to be a member of Cohen's class of time-frequency representations [27], these properties imply that CAF is very close to a low rank matrix. Thus, most of the data is concentrated in the first few singular vectors and values.

In reality, the received signals are noisy. The effect of the noise on the singular values is spread among all the singular values but, as mentioned before, most of the data is concentrated in the first few singular vectors and values. Thus, by SVD truncation we reduce the amount of noise and equivalently we increase the SNR [28]. The singular values of a sample 128 ×32 CAF are illustrated in Figure 6 for two cases: (a) noiseless signals and (b) noisy signals. As we can see, there are only 3 to 5 significant singular values in Figure 6(a) showing that the CAF is very close to a low rank matrix. But, Figure 6(b) shows that in the noisy case the number of significant singular values increases to 12. Therefore, it is clear that the signal to noise ratio can increase by

applying SVD data compression and retaining the first few singular values and discarding the rest.

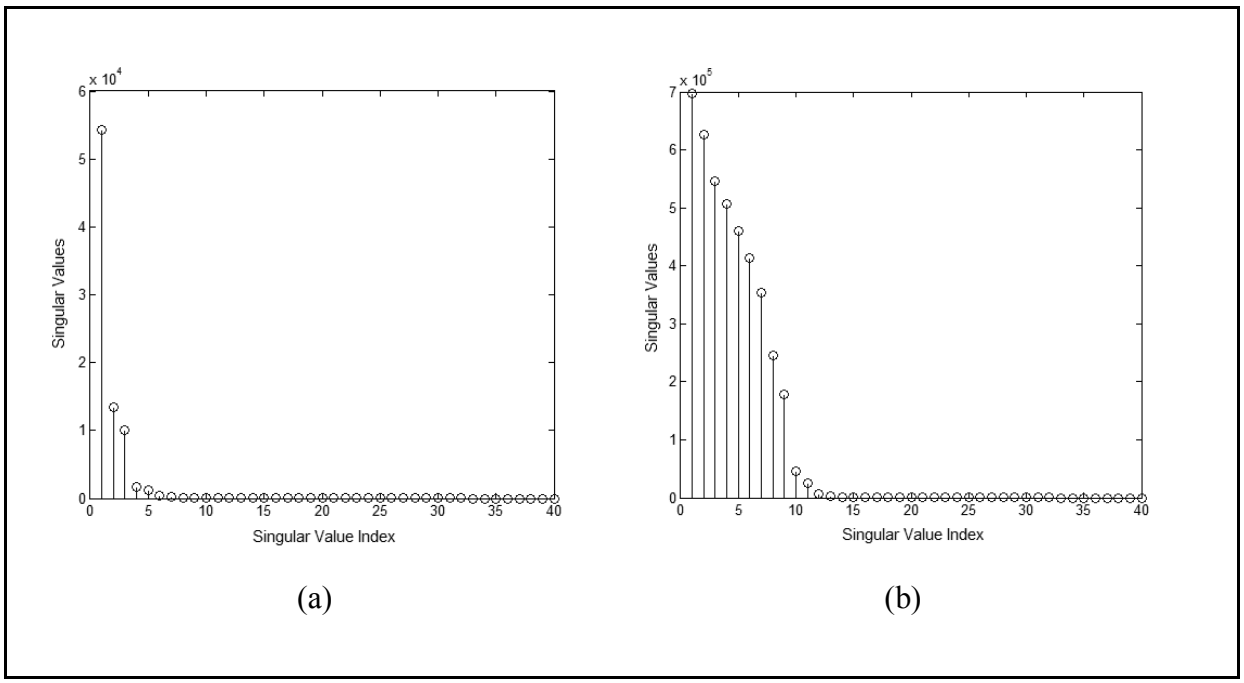

Figure 6: Singular Values of CAF: (a) Noiseless signal, (b) Noisy signal

We have applied an SVD-based data compression on CAF. The results show that SVD approach is a beneficial method for CAF data compression and also it is a strong tool for CAF denoising. Simulation results show that by applying SVD Data Compression it is possible to perform accurate location estimation in spite of the fact that we transmit fewer bits. Also for smaller compression ratio (higher bit rates), we even achieve an improvement in performance of location estimation compared to the case that we do not compress the data at all and that is because of the de-noising effect of the SVD.

We examined the performance of the proposed method using Monte Carlo computer simulations (with 500 runs each time). In this simulation, a set of 4 moving sensors and one stationary emitter are placed in a configuration as shown in Figure 7. There exists a cross ambiguity function for each two of the sensors that should be compressed and transmitted to a common site to do the location estimation. In this simulation, the signals are BPSK, the sampling frequency = 20 kHz and the number of samples is equal to 4096. Figure 8 shows the effect of data compression on RMS error. The four curves compare the cases (i) without compression, (ii) SVD-based compression with compression ratio of 25:1, (iii) SVD-based compression with compression ratio of 8:1, and (iv) SVD-based compression with compression ratio of 5:1. As we can see, even for high compression ratio of 25:1, the estimation accuracy is pretty close to the case without compression. Surprisingly, the case with the compression ratio of 5:1 (and even the case with the compression ratio of 8:1 in some points) yields more accurate results than without compression case. This improvement is obtained because of the de-noising property of SVD-

based data compression.

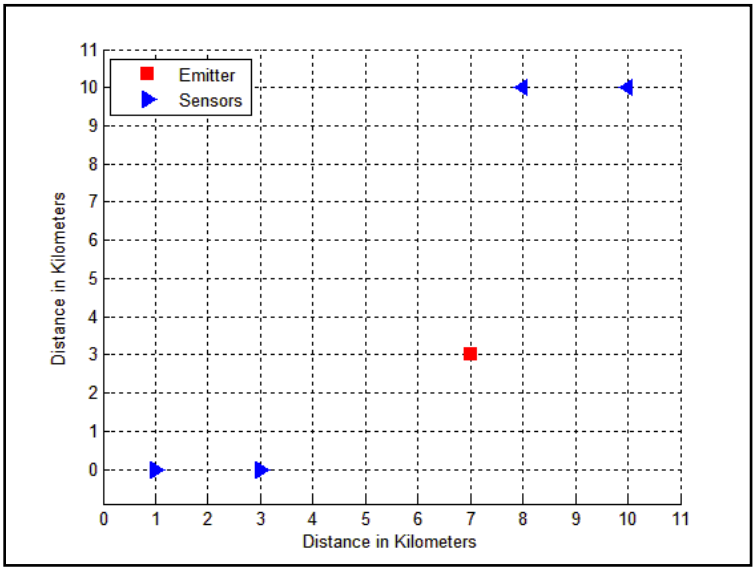

Figure 7: Placement of the sensors and the emitter position used for simulation.

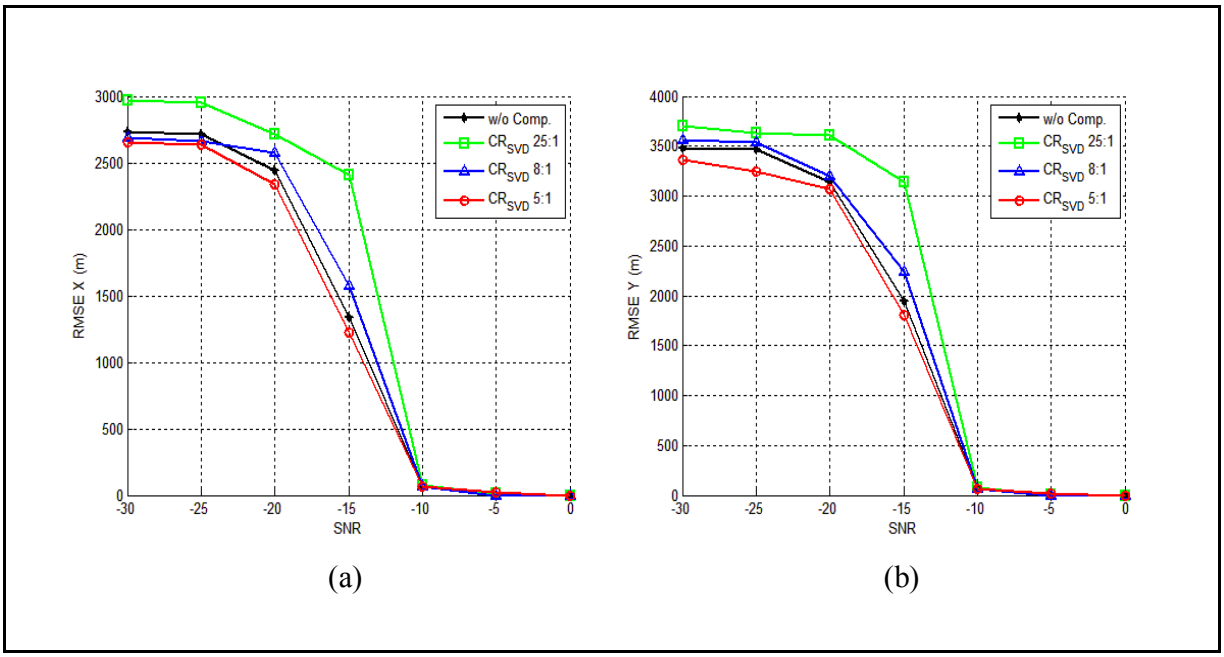

Figure 8: Location error using SVD-based CAF compression for various compression ratios.

4.1.4 Semi-Decentralized DPD

Comparing the classic method to DPD method, we can see that in classic method we only transfer the TDOA/FDOA values to the center site that leads to a very low data transmission load; but in DPD we transfer the whole received signals (or the whole CAFs as suggested in previous section) to the center site that ends up with more accurate results in localization. In this section, we develop a method taking the advantages of both classic and DPD scenarios. In fact, we use the same idea of Decentralized DPD exploiting the relationship between different CAFs to reduce the amount of data transmission in the sensor network

Suppose that two sensors *R1* and *R2* receive the LPE signals $u(t)$ and $v(t)$, respectively. Under the so-called narrowband approximation and assuming that we can estimate the antenna and electronic devices attenuations, the lowpass equivalent (LPE) model of the received signal for noise-free case will be [11]:

$$u(t) = \alpha e^{-j\omega_1 t}\hat{s}(t-\tau_1)$$
$$v(t) = \alpha e^{-j\omega_2 t}\hat{s}(t-\tau_2)$$

where τ_1 and τ_2 are the time delays and ω_1 and ω_2 are the Doppler shifts for the first and second received signals, $\alpha = e^{-j\omega_c\tau_1}$, $\beta = e^{-j\omega_c\tau_2}$ and ω_c is the carrier frequency in rad/sec [11]. Now, we can write one of the received signals in terms of the other one:

$$v(t) = u(t+\tau_{12})e^{j\omega_c\tau_{12}}e^{j\omega_{12}t}e^{j\omega_1\tau_{12}} \tag{10}$$

where $\tau_{12} = (\tau_1 - \tau_2)$ is the TDOA and $\omega_{12} = (\omega_1 - \omega_2)$ is the FDOA. Then, the CAF is:

$$\begin{aligned} CAF_{12}(\tau,\omega) &= \int_{-\infty}^{\infty} u(t)v^*(t-\tau)e^{j\omega t}dt \\ &= e^{j\omega_{12}\tau - j\omega_c\tau_{12} - j\omega_1\tau_{12}} \int_{-\infty}^{\infty} u(t)u^*(t-(-\tau_{12}+\tau))e^{j(\omega-\omega_{12})t}dt \\ &= e^{j\omega_{12}\tau - j\omega_c\tau_{12} - j\omega_1\tau_{12}} A_{11}(\tau-\tau_{12}, \omega-\omega_{12}) \end{aligned} \tag{11}$$

where the second line follows from (10) and the third line follows after defining

$$A_{11}(\tau,\omega) = \int_{-\infty}^{+\infty} u(t)u^*(t-\tau)e^{j\omega t}dt \ ,$$

which is the Auto Ambiguity function (AAF). With a similar approach for three sensors and applying (10) for the signals received by first and second receivers, we will have:

$$CAF_{23}(\tau,\omega) = e^{j(-\omega-\omega_{12}+\omega_c+\omega_1)\tau_{12}}CAF_{13}(\tau+\tau_{12}, \omega+\omega_{12}) \tag{12}$$

where CAF_{mn} is the cross ambiguity function between signals received by sensor *m* and sensor *n*. In equation (12), having (τ_{12}, ω_{12}) and one sample point of CAF_{23} and CAF_{13} it is possible to

compute ω_1. In the noisy case, the point (τ_{12},ω_{12}) can be *estimated* as the position of peak of the CAF_{12} magnitude in the (TDOA-FDOA) plane and that is why we named this method as Semi Optimal Decentralized DPD. Also, note that this estimation is applicable as long as we are able to find the peak of the CAF_{12} magnitude. Thus, having (τ_{12},ω_{12}), CAF_{13} , it is possible to reconstruct the whole CAF_{23} and we don't need to transmit the CAF_{23} to the center site anymore. Similarly, in a sensor network when L sensors receive a signal from a single emitter, we can show that:

$$CAF_{mn}(\tau,\omega) = e^{j(-\omega-\omega_{mp}+\omega_c+\omega_p)\tau_{mp}} CAF_{pn}(\tau+\tau_{mp},\omega+\omega_{mp}) \tag{13}$$

where τ_{mp} and ω_{mp} are the TDOA and FDOA between signals received by sensor p and sensor m. As a special case when $p = 1$, we have:

$$CAF_{mn}(\tau,\omega) = e^{j(-\omega-\omega_{1m}+\omega_c+\omega_1)\tau_{1m}} CAF_{1n}(\tau+\tau_{1m},\omega+\omega_{1m}) \tag{14}$$

Exploiting (14), it is possible to construct the Cross Ambiguity Matrix (CAM in [19] or Q in [9]) by transferring only the first element in each column of the matrix (in other word, by transferring the first row of the matrix) plus the corresponding TDOA/FDOAs and it leads to a large reduction in computation load and amount of data transmission.

Figure 9 illustrates a simple case of 4 receiving sensors. As we see in Figure 9(a), sensor1 (it can be obviously each of the sensors) propagates its received signal into the network. Each one of the other sensors can compute the CAF between sensor1 and itself. Then, each sensor can transmit the computed CAF to a common site (which can be one of the sensors). In Figure 9(b), we assumed sensor2 as the common point. After receiving CAF_{13} and CAF_{14} , sensor2 is able to compute CAF_{23}, having CAF_{12} (computed by itself) and CAF_{13} (received from sensor3) applying (14). It is also able to compute CAF_{24} and CAF_{34} having CAF_{12}, CAF_{13} and CAF_{14} easily. Now, sensor2 has everything to form the matrix CAM and do the location estimation. Note that according to (14), all of the CAF calculations are nothing more than delay, Doppler and phase shifts. Thus, the sensor2 does not suffer from extra CAF calculations.

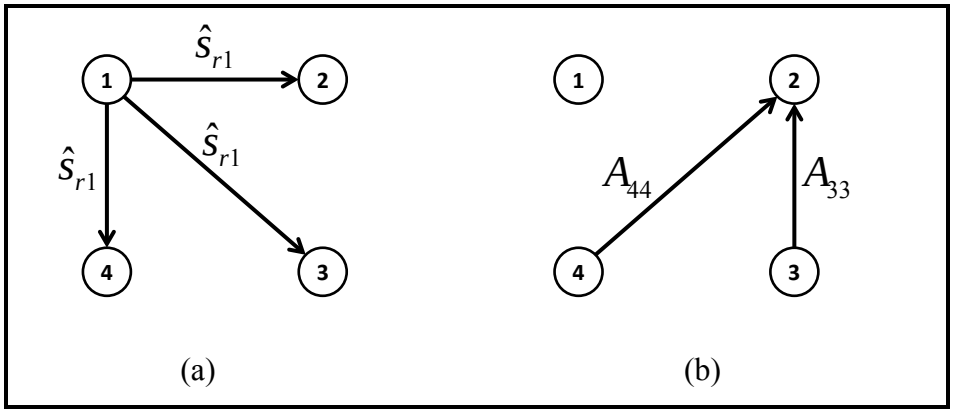

Figure 9: Semi Decentralized DPD for four receivers.

We examined the proposed method using Monte-Carlo computer simulations (with 500 runs each time). In this simulation, a set of 3 moving sensors and one stationary emitter are placed in a configuration as shown in Figure 10. In this simulation, we compute CAF_{12} and CAF_{13} directly using stein method [2] and then compute the CAF_{23} using (12). Then having all of the elements, we formed matrix CAM and apply the DPD method. The sampling frequency is 20 kHz and the number of samples is equal to 4096. Figure 11 shows the RMS error of emitter location estimation for X and Y dimensions compared to original DPD and Classic methods.

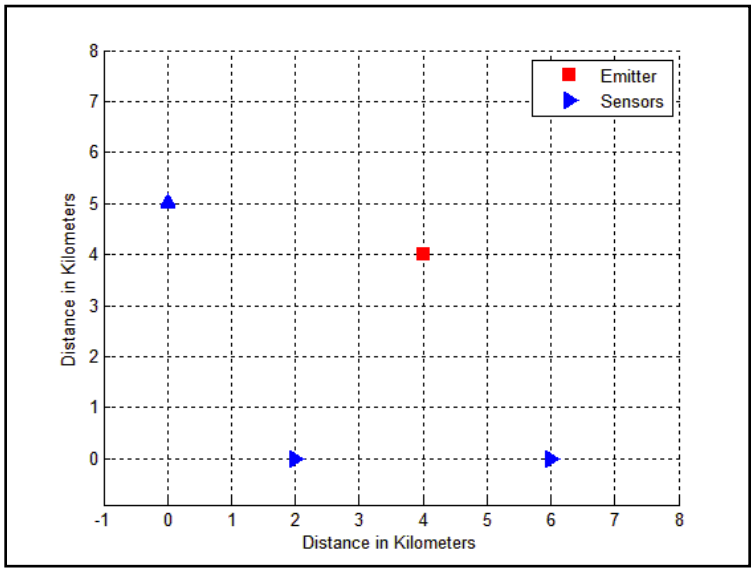

Figure 10: Placement of the sensors and the emitter position used for simulation.

Semi Decentralized DPD leads to a large reduction in computation load compared to DPD and large reduction in the amount of data transmission compared to Decentralized DPD with the cost of lower accuracy, but as we can see in Figure 11, it is still much more accurate compared to classic TDOA/FDOA method.

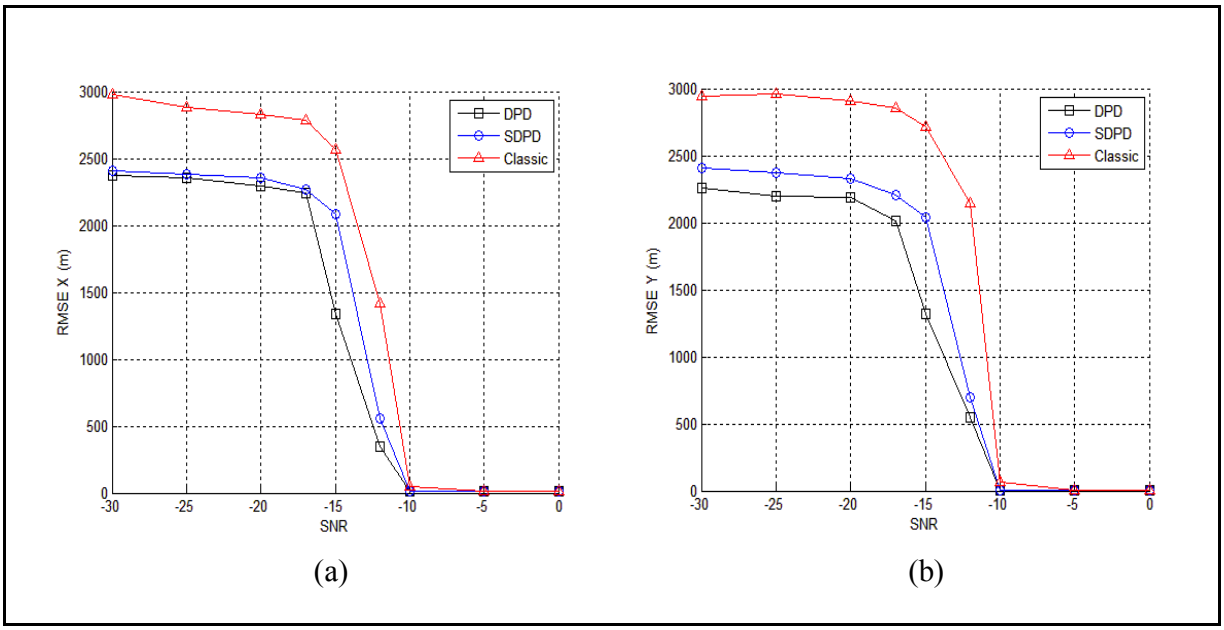

Figure 11: RMS errors for X and Y versus SNR.

4.1.5 Summary

The one-stage localization method is a major new development in TDOA/FDOA-based emitter location that provides significant improvement in performance at low SNR levels. However, that improvement comes at a cost of significantly more computational complexity. Worse, as DPD was proposed, that complexity is all concentrated at one computing node, which is different from the classical method where the computations are distributed evenly among the sensors. Furthermore, unlike the classical method, the location processing is highly complex (requiring the computation of eigenvalues for each grid point). The large amount of mathematical computations that should be done by a single center point may make some restrictions in processing. Moreover, a complete dependence of the whole process (in both data collection and data processing) on only one single point is also a problem that may reduce the reliability of the system. In this paper, we developed several methods to reduce the load of data computation and data transmission using distributed data computation and processing, applying data compression methods, exploiting the CAF properties, taking advantage of CAF relationships in the sensor network and exploiting some kind of beneficial approximations.

The *Approximated DPD* method proposed here exploits the simplicity of Gershgorin's theorem to approximately compute the largest eigenvalue without the high cost of exactly computing it. This enables each sensor to locally make its best estimate of the location based on that data it has. These locally-generated estimates are then transmitted to a central location where a final decision is made.

In *Decentralized DPD* method, we applied the distributed computation idea to divide the mathematical calculation load among all sensors of the network. In this method, we don't use any other approximation more than data compression and the quality of this method is the same as the Original DPD for proper bit rates.

Finally, in *Semi-Optimal Decentralized DPD*, we used the same idea of Decentralized DPD in addition to exploiting the relationship between different CAFs to eliminate the data redundancy and this idea leads to a large data transmission reduction.

All of the proposed methods allows DPD to be implemented in a decentralized manner where no single sensor is required to do an unfair share of the computations, yet the performance improvement of DPD is not sacrificed.

4.2 Spatial Sparsity-Based Approach to Emitter Location

Passive emitter localization is a challenging issue in statistical signal processing. The position can be estimated by measuring one or more location-dependent signal parameters. One of the most popular and common emitter location methods is based on TDOA and FDOA estimations. In the classical approach to this method, FDOA and TDOA are estimated from the cross-correlation of the signals received by several pairs of sensors [1]; this is done by computing the cross ambiguity function (CAF) [2] and finding the peak of its magnitude surface. Then these TDOA/FDOA estimates are used in statistical processing to locate the emitter [3].

However the classic two-stage method is not necessarily optimal because in the first stage of these methods, the TDOA and FDOA estimates are obtained by ignoring the fact that all measurements should be consistent with a single emitter location [9]. In other words, each stage is itself optimal but the cascade of the two stages is not necessarily optimal.

In this section, we exploit spatial sparsity of the emitter on the x-y plane and use convex optimization theory to estimate the location of the emitter directly without going through the intermediate stage of TDOA/FDOA estimation. It is obvious that in emitter location problems, the number of emitters is much smaller than the number of all grid points in a fine grid on the x-y plane. Thus, by assigning a positive number to each one of the grid points containing an emitter and assigning zero to the rest of points, we will have a very sparse grid plane matrix that can be reformed as a sparse vector. Since each element of this vector corresponds to one grid point in the x-y plane, we can estimate the location of emitters by extracting the position of non-zero elements of the sparsest vector that satisfies the TDOA/FDOA relationship between transmitted signals and received signals. In principle, sparsity of the grid vector can be enforced by minimizing its ℓ_0-norm (i.e., the number of non-zero elements in the grid vector). However, since the ℓ_0-norm minimization is an NP-hard non-convex optimization problem, it is very common (e.g in compressive sensing problems) to approximate it with ℓ_1-norm minimization, which is a convex optimization problem and also achieves the sparse solution very well [30]. Thus, after formulating the problem in terms of the sparse grid vector, we can estimate this vector by pushing sparsity using ℓ_1-norm minimization on the grid vector, subject to the TDOA/FDOA relationship between the signals transmitted from the grid point and the signals received by the sensors.

In [31], the authors suggested a source localization method based on TDOA in a multipath channel exploiting the sparsity of the multipath channel for estimation of the line-of-sight component. In this method, the sensors don't need to know the information on the specific transmitted symbols but, they require knowledge of the pulse shape of the transmitted signal. In [32], the authors suggested a compressive-sensing based distributed target localization using TDOA. In this method, each sensor approximates the transmitted signal by its own received

signal mapped to each one of the grid points. This idea helps to reduce the amount of data transmission in the sense of distributed localization but it lowers the quality of the estimation since each sensor estimates the transmitted signal just using its own received signal. Also, each sensor computes its own location estimation that is not necessarily equal to other sensors' estimations. Weiss and Amar [7], [8], [9] developed a single-stage Least-Squares method using TDOA and FDOA, named direct position determination (DPD). Vankayalapati and Kay [19] also derived similar results based on a detection theory point of view; the DPD estimator was derived as the ML estimator needed for the generalized likelihood ratio detector. The performance of the DPD method is better than the two-stage classic method (especially for low SNRs). However, the simulation results show that DPD does not obtain accurate results in the case of multipath or multi-emitter scenarios.

In this paper, contrary to [31] and [32], we developed a method based on both TDOA and FDOA to take advantage of both delay and Doppler shifts. Contrary to [6], our method does not need any knowledge of the transmitted signal's pulse shape nor any other *a priori* information. Similar to [32], we exploit the grid point spatial sparsity but, we consider the transmitted signal as a *deterministic unknown signal* that will be estimated in the sensor network using all received signals. Similar to [19] and [9], we estimate the emitter location directly without going through the intermediate stage of TDOA/FDOA estimation. However, the Monte-Carlo simulation results show the higher performance of the proposed method compared to DPD method and classic two-stage method especially in multipath scenarios.

Suppose that an emitter transmits a signal and L sensors receive that signal. The complex baseband signal observed by the lth sensor is

$$r_l(t) = \alpha_l s(t-\tau_l) e^{j2\pi f_l t} + w_l(t) \tag{15}$$

where $s(t)$ is the transmitted signal, α_l is the complex path attenuation, , f_l is the Doppler shift, τ_l is the signal delay and $w_l(t)$ is a white, zero mean, complex Gaussian noise. Assume that each sensor collects N_s signal samples at sampling frequency $F_s = 1/T_s$. Then, we have

$$\boldsymbol{r}_l = \alpha_l \boldsymbol{W}_l \boldsymbol{D}_l \boldsymbol{s} + \boldsymbol{w}_l \tag{16}$$

with

$$\begin{aligned}
\boldsymbol{s} &= [s(t_1), \quad s(t_2), \quad \ldots \quad , \quad s(t_{Ns})]^T \\
\boldsymbol{r}_l &= [r_l(t_1), \quad r_l(t_2), \quad \ldots \quad , \quad r_l(t_{Ns})]^T \\
\boldsymbol{w}_l &= [w_l(t_1), \quad w_l(t_2), \quad \ldots \quad , \quad w_l(t_{Ns})]^T \\
\boldsymbol{W}_l &= diag\{e^{j2\pi f_l t_1}, \quad e^{j2\pi f_l t_2}, \quad \ldots \quad , \quad e^{j2\pi f_l t_{Ns}}\}
\end{aligned}$$

where $\boldsymbol{r}_l$ is the vector containing N_s samples of the received signal by lth sensor, $\boldsymbol{s}$ is N_s samples of the transmitted signal, f_l is the Doppler shift and $\boldsymbol{D_l}$ is the time sample shift operator by $n_l = (\tau_l / T_s)$ samples. We can write $\boldsymbol{D}_l = \boldsymbol{D}^{n_l}$ where $\boldsymbol{D}$ is an $N_s \times N_s$ permutation matrix defined as $[\boldsymbol{D}]_{ij} = 1$ if $i = j+1$, $[\boldsymbol{D}]_{0,N-1} = 1$ and $[\boldsymbol{D}]_{ij} = 0$ otherwise.

$$\boldsymbol{D}=\begin{bmatrix}0 & & & 1\\ 1 & 0 & & \\ & \ddots & \ddots & \\ 0 & & 1 & 0\end{bmatrix}\quad,\quad \boldsymbol{D}_l=\begin{bmatrix}0 & & & 1\\ 1 & 0 & & \\ & \ddots & \ddots & \\ 0 & & 1 & 0\end{bmatrix}^{n_l}$$

Now, we assign a number $z_{x,y}$ to each one of the grid points (x,y). Assume that $z_{x,y}$ is one for the grid points containing an emitter and zero for the rest of the grid points. Thus, the signal vector received by lth sensor will be

$$\boldsymbol{r}_l=\sum_x\sum_y z_{x,y}\alpha_{l,x,y}\boldsymbol{W}_{l,x,y}\boldsymbol{D}_{l,x,y}\,\boldsymbol{s}+\boldsymbol{w}_l, \tag{17}$$

where $\boldsymbol{W}_{l,x,y}$ and $\boldsymbol{D}_{l,x,y}$ are the Doppler shift and time sample shift operators w.r.t sensor l assuming that the emitter is located in the grid point (x,y) and the summations are over all grid points in the desired (x,y) range. Now, if we reform all of the grid points in a column vector and re-arrange the indices, we will have

$$\boldsymbol{r}_l=\sum_{n=1}^{N} z_n\alpha_{l,n}\boldsymbol{W}_{l,n}\boldsymbol{D}_{l,n}\,\boldsymbol{s}+\boldsymbol{w}_l. \tag{18}$$

In (18), we consider the transmitted signal $\boldsymbol{s}$ as a *deterministic unknown* signal (a common signal model in localization problems). Then, for each grid point, we estimate the transmitted signal using the Minimum Variance Unbiased estimator (MVU) as

$$\hat{\boldsymbol{s}}_n=\frac{1}{L}\sum_{l=1}^{L}\boldsymbol{D}_{l,n}{}^{-1}\boldsymbol{W}_{l,n}{}^{-1}\boldsymbol{r}_l, \tag{19}$$

where $\hat{\boldsymbol{s}}_n$ is the MVU estimate for the transmitted signal from grid point n.

We define the matrix $\boldsymbol{\Gamma}_n$ as the Doppler and delay operator w.r.t all L sensors, assuming that the received signal comes from the grid point n (there is an emitter at grid point n):

$$\boldsymbol{\Gamma}_n=\begin{bmatrix}\alpha_{1,n}\boldsymbol{W}_{1,n}\boldsymbol{D}_{1,n}\\ \alpha_{2,n}\boldsymbol{W}_{2,n}\boldsymbol{D}_{2,n}\\ \vdots\\ \alpha_{L,n}\boldsymbol{W}_{L,n}\boldsymbol{D}_{L,n}\end{bmatrix}_{LN_s\times N_s}.$$

Then, we can define $\boldsymbol{\theta}_n, n\in\{1,2,\ldots,N\}$ as an $LN_s\times 1$ vector containing all signals received by all L sensors when the emitter is in grid point n as

$$\boldsymbol{\theta}_n = \boldsymbol{\Gamma}_n \times \hat{\boldsymbol{s}}_n. \tag{20}$$

If we arrange all vectors $\boldsymbol{\theta}_n$ for n:1...N as the columns of a matrix $\boldsymbol{\Theta}$ as

$$\boldsymbol{\Theta} = [\boldsymbol{\theta}_1 \quad \boldsymbol{\theta}_2 \quad \dots \quad \boldsymbol{\theta}_N]_{LN_s \times N}, \tag{21}$$

and then, we have

$$\boldsymbol{r} = \boldsymbol{\Theta} \times \boldsymbol{z} + \boldsymbol{w} \tag{22}$$

with

$$\boldsymbol{r} = [\boldsymbol{r}_1^T \quad \boldsymbol{r}_2^T \quad \dots \quad \boldsymbol{r}_L^T]^T_{LN_s \times 1}$$

$$\boldsymbol{z} = [z_1 \quad z_2 \quad \dots \quad z_N]^T_{N \times 1},$$

where $\boldsymbol{r}$ is the vector of all L received signals, $\boldsymbol{z}$ is the sparse vector of z-values assigned to each grid point and $\boldsymbol{w}$ is the noise. Now, we can solve our problem by forming a *BPIC* (*Basis Pursuit with Inequality Constraints*) *problem* [33] as following:

$$\begin{cases} \hat{\boldsymbol{z}} = \arg\min \|\boldsymbol{z}\|_1 \\ s.t \quad \|\boldsymbol{\Theta} \times \boldsymbol{z} - \boldsymbol{r}\|_2 \le \varepsilon \end{cases} \tag{23}$$

or regularized *BPDN* (*Basis Pursuit Denoising*) *problem* [33] as:

$$\hat{\boldsymbol{z}} = \arg\min \|\boldsymbol{\Theta} \times \boldsymbol{z} - \boldsymbol{r}\|_2 + \lambda \|\boldsymbol{z}\|_1 \tag{24}$$

We examined the performance of the proposed method and compared the results using Monte-Carlo computer simulations for different scenarios. In the first simulation, we assumed that 3 moving sensors receive the signal from one stationary emitter placed in a configuration as shown in Figure 12 (the location of the emitter has been chosen randomly). In this simulation, the sampling frequency is 80 kHz and the number of samples is equal to 1024. In Figure 13, we can see the RMS Error vs. SNR (with 500 runs for each SNR) for estimating the location of the emitter in $(x-y)$ plane. As we see, the proposed method has better performance compared to DPD and Classic methods.

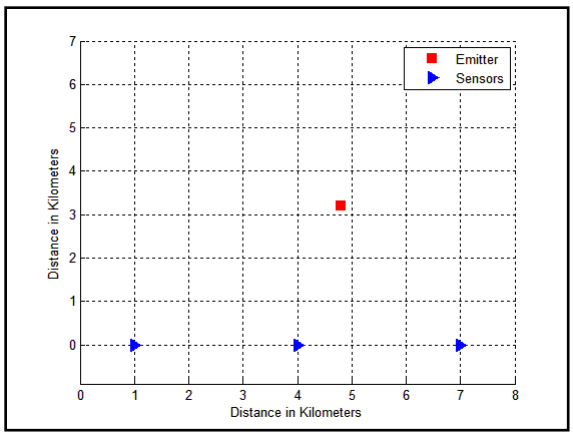

Figure 12: Placement of the sensors and the emitter position used for simulation.

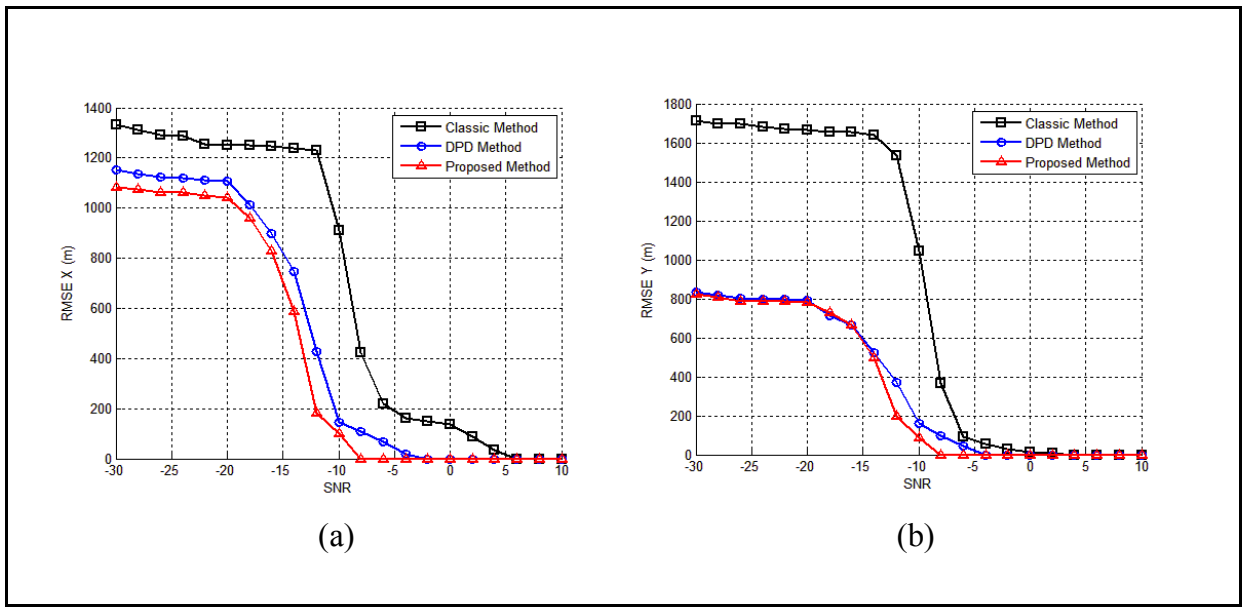

Figure 13: Location error versus SNR for single-emitter single-path case.

One of the challenging topics in source localization problems is emitter location estimation in the presence of multipath reflections. We evaluated the capability of the proposed method in dealing with multipath scenarios using Monte-Carlo simulation. In this simulation, we assumed that 4 moving sensors receive the signal from one stationary emitter placed in a configuration as shown in Figure 14 (the location of the emitter has been chosen randomly). Figure 15 shows the RMS Error vs. SNR (with 500 runs for each SNR) for estimating the location of the emitter in multipath case. The following plots show better accuracy of the proposed method over DPD and Classic methods. As we see, none of the DPD and Classic methods provide unbiased estimates for higher SNRs.

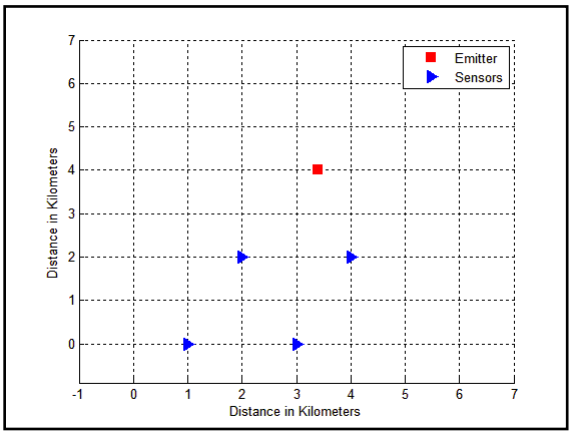

Figure 14: Placement of the sensors and the emitter position used for simulation.

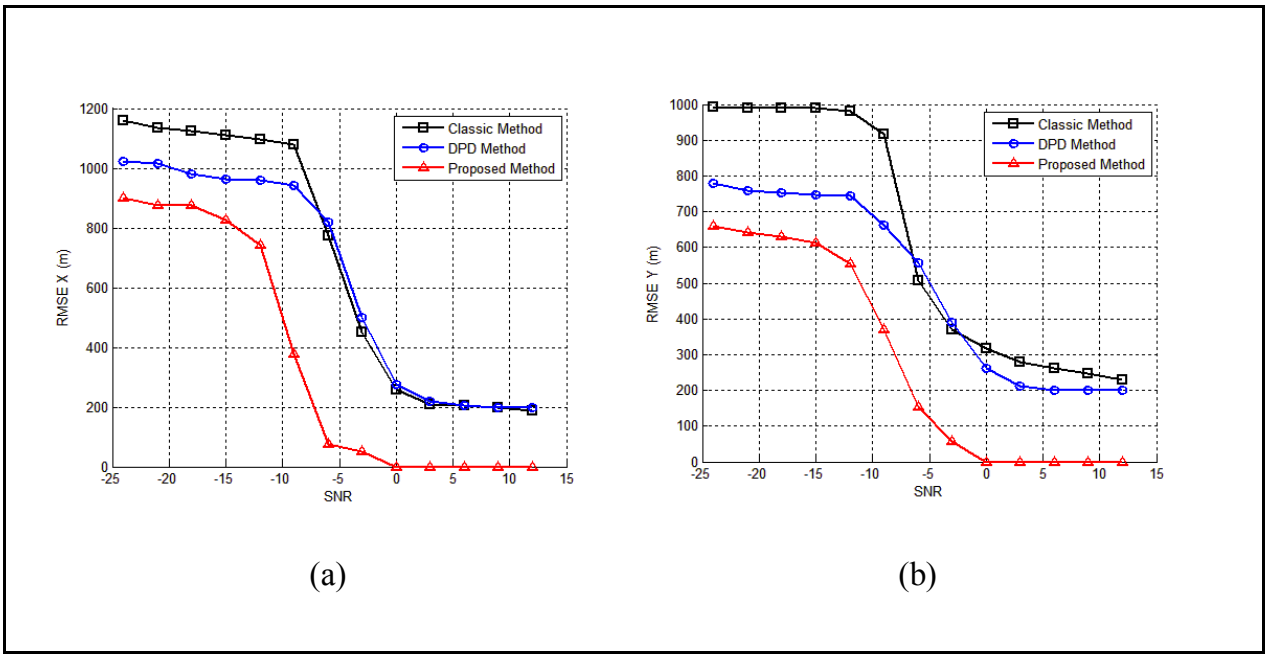

Figure 15: Location error versus SNR for multipath scenario.

In another simulation, we evaluated the performance of the proposed method and compared the results to DPD and Classic method for multi-emitter scenarios when we have more than one transmitter in the range of interest and we aim to estimate the location of all emitters. In this simulation, we assumed that 6 moving sensors receive the signal from two stationary emitters placed in the configuration as shown in Figure 16 (the location of the emitters has been chosen randomly). Figure 17 shows the RMS Error vs. SNR (with 500 runs for each SNR) for estimating the location of two emitters. Comparing the RMS Error curves, we see that the proposed method achieves much better accuracy with significantly smaller error compared to DPD and Classic methods. As we see, similar to multipath case, both DPD and Classic methods provide biased estimates at high SNRs.

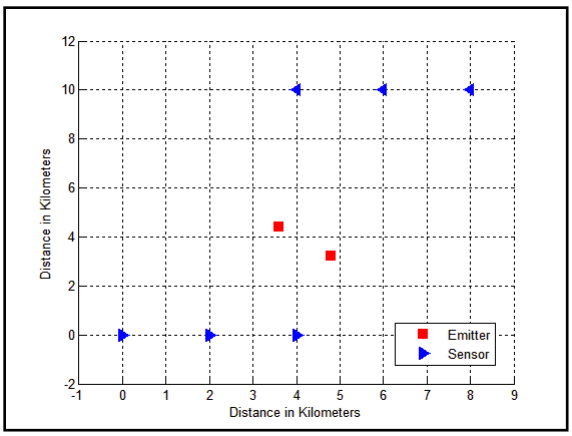

Figure 16: Placement of the sensors and the emitter position used for simulation.

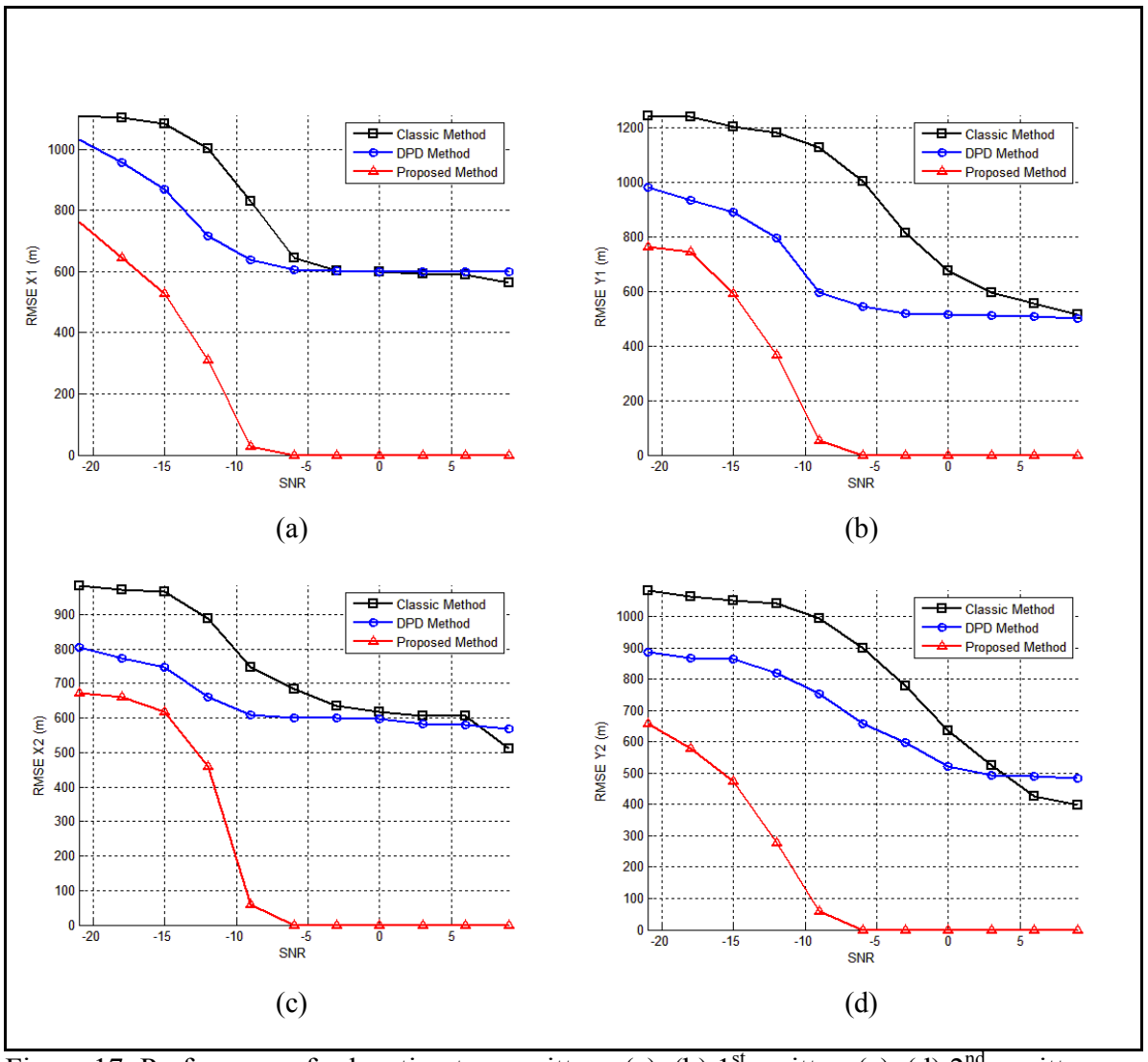

Figure 17: Performance for locating two emitters. (a), (b) 1st emitter; (c), (d) 2nd emitter.

We developed a one-stage TDOA/FDOA localization method based on spatial sparsity of emitters. In this method, we assign a non-zero number to each one of the grids containing an emitter and zero to the rest of the grid points. Thus, the vector formed from these numbers will be a sparse unknown vector that we aim to estimate. Since each element of this vector corresponds to one grid point in (x,y) plane, we can estimate the location of emitters by extracting the position of non-zero elements of the sparsest vector that satisfy the TDOA/FDOA relationship between transmitted signals and received signals. We evaluated the performance of the proposed method using Monte-Carlo simulation. Comparing the three curves in each plot in Figure 13, Figure 15 and Figure 17 shows that the proposed method has better performance (especially in multi-path and multi-emitter cases) compared to direct position determination (DPD) and two-stage Classic localization methods. Simulation results show that contrary to DPD and Classic methods, the proposed method is a very reliable and strong tool to deal with multipath and multi-emitter scenarios.

5.0 CONCLUSIONS

For several decades now emitter location has been done using a two-stage approach but recently it has been shown that a single-stage method (called DPD) has some performance advantages. However, this comes at the cost of some difficulties that hinder easy implementation. In particular, the original formulation of DPD calls for the transmission of all signals to a single sensor. This causes several problems: (i) communication limitations restrict transmission of all data to a single sensor, (ii) all computation is performed at a single sensor – resulting in an excessive burden for one sensor and (iii) if that single computing sensor is prevented from completing the location (due to failure or enemy action) then no location can be made available. The first set of results provided here address these issues and make strides toward a feasible implementation of the DPD method – thus helping to make DPD's improved performance more readily available in practice.

However, in scenarios of multipath and multiple co-channel emitters we demonstrated that even though the DPD method does improve upon the classical methods it still leaves a need for further improvement. We showed that it is possible to implement a single-stage method that is similar to DPD but that also exploits the sparsity of emitters in space. The simulation results showed that this method significantly improves the performance buy at least 2 orders of magnitude! This is a tremendous improvement and – once developed to be feasible in the real world – will provide accurate locations in environments previously found to be unworkable.

6.0 REFERENCES

[1] S. Stein, "Differential delay/Doppler ML estimation with unknown signals," *IEEE Transactions Signal Processing.*, 41(8), 2717–2719 (1993).

[2] S. Stein, "Algorithms for Ambiguity Function Processing," *IEEE Transactions on Acoustics, Speech, and Signal Processing*, 29(3), 588-599 (1981).

[3] D. J. Torrieri, "Statistical theory of passive location system," *IEEE Transactions on Aerospace and Electronic Systems,* vol. AES-20, no. 2, March 1984, pp. 183 – 198.

[4] M. L. Fowler and M. Chen, "Fisher-Information-Based Data Compression for Estimation Using Two Sensors," *IEEE Transactions on Aerospace and Electronic Systems,* vol. 41, no. 3, July 2005, pp. 1131 - 1137.

[5] M. Chen and M. L. Fowler, "Data Compression for Multiple Parameter Estimation with Application to Emitter Location Systems," *IEEE Transactions on Aerospace and Electronic Systems,* vol. 46, no. 1, January 2010, pp. 308 – 322.

[6] G. D. Hartwell, "Improved Geo-Spatial Resolution Using a Modified Approach to the Complex Ambiguity Function (CAF)", Master's Thesis, Naval Postgraduate School (2005).

[7] A. Weiss, "Direct Position Determination of Narrowband Radio Frequency Transmitters," *IEEE Transactions Signal Process.* , 11(5), 513-516 (2004).

[8] A. Amar and A. Weiss, "Localization of Narrowband Radio Emitters Based on Doppler Frequency Shifts," *IEEE Transactions Signal Process.* , 56(11), 5500-5508 (2008).

[9] A. Weiss and A. Amar, "Direct Geolocation of Stationary Wide Band Radio Signal Based on Delays and Doppler Shifts," *IEEE Workshop on Statistical Signal Processing,* Aug. 31 – Sept. 3, 2009, Cardiff, Wales, UK.

[10] J. M. Shapiro, "Embedded image coding using zerotrees of wavelet coefficients," *IEEE Transactions on Signal Processing,* 41(12), 3445-3462 (1993).

[11] R. E. Blahut, "Theory of remote surveillance algorithms," in The IMA Volumes in Mathematics and Its Application, Volume 32, Radar and Sonar, 1991.

[12] R. Price and E. M. Hofstetter, "Bounds on the Volume and Height Distributions of the Ambiguity Function," *IEEE Transaction on Information Theory,* vol. 11, Apr 1965, pp. 207 – 214.

[13] C. H. Wilcox, "The synthesis problem for radar ambiguity functions," in The IMA Volumes in Mathematics and Its Application, Volume 32, Radar and Sonar, 1991.

[14] C. E. Cook and M. Bernfeld ; *Radar Signals, An Introduction to Theory and Application*; 1993 Artech House, Inc.

[15] F. Reis, "A linear transformation of the ambiguity function plane," *IEEE Transactions on Information Theory*, IRE, vol. 8, Jan 1962, pp. 59-59.

[16] C. Stutt, "Some Results on Real-Part/Imaginary-Part and Magnitude-Phase Relations in Ambiguity Functions," *IEEE Transaction on Information Theory,* vol. 10, Oct 1964, pp. 321-327.

[17] C. Darmet, J. Gauthier, and F. Gourd, "Elliptic and Almost Hyperbolic Symmetries for the Woodward Ambiguity Function, " *IEEE Transaction on Information Theory,* vol. 37, Sep 1991, pp. 1388-1398.

[18] J. Donohoe and F. M. Ingels, "The Ambiguity Properties of FSK/PSK Signals," *IEEE international Radar Conference.* May 1990, pp. 268 – 273.
[19] N. Vankayalapati and S. Kay, "Asymptotically Optimal Localization of an Emitter of Low Probability of Intercept Signals Using Distributed Sensors," *IEEE Transactions on Aerospace and Electronic Systems,* vol. 48, no. 1, Jan. 2012.
[20] M. Wax, "The joint estimation of differential delay, Doppler and phase," *IEEE Trans. Inf. Theory*, vol. IT-28, pp. 817–820, Sep. 1982.
[21] M. L. Fowler and X. Hu, "Signal models for TDOA/FDOA estimation," *IEEE Trans. Aerosp. Elect. Sys.*, vol. 44, pp. 1543–1549, Oct. 2008
[22] A. Yeredor and E. Angel, "Joint TDOA and FDOA Estimation: A Conditional Bound and Its Use for Optimally Weighted Localization", *IEEE Transactions on Signal Processing,* Vol. 59, No. 4, APR. 2011
[23] T. K. Moon and W.C. Stirling, Mathematical Methods and Algorithms for Signal Processing, Prentice-Hall, 2000.
[24] L. L. Scharf, "The svd and reduced-rank signal processing," *SVD and Signal Processing II, Algorithms, Analysis and Applications*, pp. 4–25, 1991.
[25] E. Biglieri and K. Yao, "Some properties of singular value decomposition and their applications to digital signal processing," *Signal Processing*, vol. 18, no. 3, pp. 277–89, Nov. 1989.
[26] C. Heil , J. Ramanathan and P. Topiwala, "Asymptotic Singular Value Decay of Time-Frequency Localization Operators", Wavelet Applications in Signal and Image Processing II, SPIE, 1994.
[27] L. Cohen, "Time-Frequency Analysis," *Prentice-Hall*, New York, 1995.
[28] M.L. Fowler, M. Chen, J. A. Johnson, and Z. Zhou, "Data compression using SVD and Fisher information for radar emitter location", *Signal Processing Journal*, Vol. 90 Issue 7, July, 2010.
[29] M. Marcus and H. Minc, "A Survey of Matrix Theory and Matrix Inequalities", Dover Publication, 1992.
[30] R. G. Baraniuk. "Compressive Sensing". *IEEE Signal Processing Magazine*, 118–120, July 2007.
[31] C.R. Comsa, A.M. Haimovich, S. Schwartz, Y. Dobyns and J.A. Dabin,"Source Localization Using Time Difference Of Arrival Within A Sparse Representation Framework", *International Conference on Acoustic, Speech and Signal Process.(ICASP),* May 22–27, 2011.
[32] V. Cevher, M. F Duarte and R. G Baraniuk, "Distributed Target Localization Via Spatial Sparsity", 16th European Signal Processing Conference, Switzerland, Aug 2008.
[33] M. F. Duarte and Y. C. Eldar, "Structured Compressed Sensing: From Theory to Applications", *IEEE Transactions on Signal Process.* , 4053 - 4085, 2011.
[34] Stephen Boyd, Lieven Vandenberghe, "Convex Optimization", Cambridge University Press, 2009.

APPENDIX

As mentioned above, we can consider the CAF as an image and we can apply image compression methods to compress it. However, not all of the CAF points have the same importance for location estimation, thus it is possible to assign different weights to different CAF points and therefore allocate larger number of data bits to transmit the more significant area, which contains the mainlobe area.

Price and Hofstetter [12] have done detailed research on the bounds of the ambiguity function volume distribution. Wilcox [13] showed that the contour of ambiguity function magnitude close to the peak is always an ellipse. This contour can be formed by the intersection of the mainlobe magnitude and a level plane. It is possible to find the approximate equation of this ellipse in terms of signal bandwidth, signal duration, signal energy and a specific level. The width of this ellipse along the TDOA axis is proportional to the reciprocal of the signal's rms bandwidth; likewise, the width of the ellipse along the FDOA axis is proportional to the reciprocal of signal's rms duration [14]:

$$\Delta\tau \propto (1/B_{rms})$$

$$\Delta\omega \propto (1/T_{rms})$$

where B_{rms} is rms value of signal bandwidth and T_{rms} is rms value of signal duration.

Thus, it is possible to determine the approximate significant area which is more important for the purpose of location estimation. Note that it is always possible to rotate the ambiguity function when it is tilted. An interesting property of ambiguity function is that the new function under the transformation that rotates the $\tau - \omega$ plane through some angle θ will be another ambiguity function. This new ambiguity function is corresponding to the new signals which are related to the old signals and the angle θ [14],[15].

Under the so-called narrowband approximation the lowpass equivalent (LPE) model of the received signal will be:

$$\hat{s}_r(t) = e^{-jw_c\tau_d}\, e^{-jw_d t}\, \hat{s}(t-\tau_d) \tag{A1}$$

where $\hat{s}(t)$ is the LPE of the transmitted signal, w_d is the Doppler and τ_d is the delay for the received signal [11]. Now, suppose that two sensors Rx1 and Rx2 receive the LPE signals $\hat{s}_{r1}(t)$ and $\hat{s}_{r2}(t)$, respectively. The ML estimate for TDOA and FDOA can be obtained using the magnitude of the CAF:

$$A_{12}(\tau,\omega) = \int_{-\infty}^{+\infty} \hat{s}_{r1}(t)\hat{s}_{r2}{}^{*}(t-\tau)e^{j\omega t}dt \tag{A2}$$

which measures the correlation between $\hat{s}_{r1}(t)$ and a Doppler-shifted by ω and delayed by τ version of $\hat{s}_{r2}(t)$.

The auto ambiguity function (AAF) (or just ambiguity function as in some papers) is defined as:

$$A_{uu}(\tau,\omega) = \int_{-\infty}^{+\infty} u(t)u^*(t-\tau)e^{j\omega t}dt \tag{A3}$$

where $u(t)$ can be the LPE signal. In fact, auto ambiguity function shows the correlation between a signal and a Doppler-shifted by ω and delayed by τ version of itself. It is straight forward to show that AAF has a kind of symmetry around the origin [13], [14], [16].

$$A_{uu}(-\tau,-\omega) = A_{uu}^*(\tau,\omega)\, e^{j\tau\omega} \tag{A4}$$

$$|A_{uu}(-\tau,-\omega)| = |A_{uu}(\tau,\omega)|$$

where $A_{uu}^*(\tau,\omega)$ is the complex conjugate of AAF and $|A_{uu}(\tau,\omega)|$ is the magnitude of AAF.

It is also simple to prove a similar property for CAF [14],[16]:

$$A_{uv}(-\tau,-\omega) = A_{vu}^*(\tau,\omega)\, e^{j\tau\omega}$$

$$|A_{uv}(-\tau,-\omega)| = |A_{vu}(\tau,\omega)|$$

where $A_{uv}(\tau,\omega)$ is the CAF between signal $u(t)$ and $v(t)$. However, $A_{vu}(\tau,\omega)$ is the CAF between arbitrary signals $v(t)$ and $u(t)$, not specifically related by delay and Doppler to a single transmitted signal. To develop a result that we can exploit for our purpose we explore a similar result for the case when the signals are received from a transmitter. Then (A1) gives

$$u(t) = e^{-j\omega_c\tau_1}\, e^{-j\omega_1 t}\, \hat{s}(t-\tau_1)$$

$$v(t) = e^{-j\omega_c\tau_2}\, e^{-j\omega_2 t}\, \hat{s}(t-\tau_2)$$

where τ_1 and τ_2 are the time delays and ω_1 and ω_2 are the Doppler shifts for the first and second received signals. Now, we can write one of them in terms of the other one,

$$v(t) = u\big(t+\tau_p\big)e^{j\omega_c\tau_p}\; e^{j\omega_p t}\, e^{j\omega_1\tau_p} \tag{A5}$$

where $\tau_p = (\tau_1 - \tau_2)$ is the TDOA and $\omega_p = (\omega_1 - \omega_2)$ is the FDOA.

$$A_{uv}(\tau,\omega) = \int_{-\infty}^{+\infty} u(t)v^*(t-\tau)e^{j\omega t}dt \quad \overset{(A5)}{\Longrightarrow}$$

$$= e^{j\omega_p\tau - j\omega_c\tau_p - j\omega_1\tau_p} \int_{-\infty}^{+\infty} u(t)u^*\big(t-(-\tau_p+\tau)\big)\, e^{j(\omega-\omega_p)t}dt$$

$$= \left[e^{j\omega_p\tau - j\omega_c\tau_p - j\omega_1\tau_p}\right] A_{uu}\big(\tau-\tau_p, \omega-\omega_p\big) \tag{A6}$$

Thus, the CAF is rewritten in terms of AAF. Then, by replacing the τ by $(\tau+\tau_p)$ and ω by $(\omega-\omega_p)$, the following equations are concluded,

$$A_{uv}(\tau+\tau_p,\omega+\omega_p) = e^{j\omega_p(\tau+\tau_p)-j\omega_c\tau_p-j\omega_1\tau_p}\, A_{uu}(\tau,\omega) \tag{A7}$$

$$A^*_{uu}(\tau,\omega) = e^{j\omega_p(\tau+\tau_p)-j\omega_c\tau_p-j\omega_1\tau_p}\, A^*_{uv}(\tau+\tau_p,\omega+\omega_p) \tag{A8}$$

Now, by negating the τ and ω in (A7), we have:

$A_{uv}(-\tau+\tau_p,-\omega+\omega_p) =$

$\overset{(A7)}{\Longrightarrow} = [e^{j\omega_p(-\tau+\tau_p)-j\omega_c\tau_p-j\omega_1\tau_p}]\, A_{uu}(-\tau,-\omega)$

$\overset{(A4)}{\Longrightarrow} = \left[e^{j\omega_p(-\tau+\tau_p)-j\omega_c\tau_p-j\omega_1\tau_p}\ e^{-j\omega\tau}\right] A^*_{uu}(\tau,\omega)$

$\overset{(A8)}{\Longrightarrow} = \left[e^{j\omega_p(-\tau+\tau_p)-j\omega_c\tau_p-j\omega_1\tau_p}\ e^{-j\omega\tau}\, e^{j\omega_p(\tau+\tau_p)-j\omega_c\tau_p-j\omega_1\tau_p}\right] A^*_{uv}(\tau+\tau_p,\omega+\omega_p)$

$= [e^{(j2\omega_p\tau_p-j2\omega_c\tau_p-j2\omega_1\tau_p)}\ e^{-j\omega\tau}]\, A^*_{uv}(\tau+\tau_p,\omega+\omega_p)$

$= e^{-j(\omega\tau+\beta)}\, A^*_{uv}(\tau+\tau_p,\omega+\omega_p)$

where β is defined as $(2\omega_p\tau_p - 2\omega_c\tau_p - 2\omega_1\tau_p)$ and finally,

$$A_{uv}(-\tau+\tau_p,-\omega+\omega_p) = \ e^{-j(\omega\tau+\beta)}\, A^*_{uv}(\tau+\tau_p,\omega+\omega_p) \tag{A9}$$

and

$$|\, A_{uv}(-\tau+\tau_p,-\omega+\omega_p)\,| \ = |\, A_{uv}(\tau+\tau_p,\omega+\omega_p)\,| \tag{A10}$$

which is the symmetry property we can exploit for data compression. This result provides a kind of symmetry of the CAF around the point (τ_p,ω_p) or the peak of CAF magnitude.

Now, it is possible to exploit this property in data compression. In practice, the received signals $u(t)$ and $v(t)$ are the delayed and Doppler-shifted version of transmitted signal plus noise. This noise perturbs the CAF a little bit from the perfect symmetry.

Thus, we rewrite (A10) as,

$$|\, A_{uv}(-\tau+\tau_p,-\omega+\omega_p)\,| \ = |\, A_{uv}(\tau+\tau_p,\omega+\omega_p)\,| \ + \ E \tag{A11}$$

where *E* can be the error from perfect symmetry which is a negligible value. Thus, using the symmetry property, it is possible to extract the entire CAF magnitude by transmission of only half of the CAF magnitude plus the small residual amount of *E*. In this scheme we apply the EZW data compression method on only half of CAF as well as on *E*.

LIST OF SYMBOLS, ABBREVIATIONS AND ACRONYMS

AAF	auto ambiguity function
ADC	analog-to-digital converter
AESA	active electronically scanned array
BPDN	basis pursuit denoising
BPIC	basis pursuit with inequality constraints
BPSK	binary phase shift keying
CAF	cross-ambiguity function
CAM	cross ambiguity matrix
COMINT	communication intelligence
COTS	commercial-off-the-shelf
CRLB	Cramer-Rao lower bound
DAWG	digital arbitrary waveform generator
DPD	direct position determination
ELINT	electronics intelligence
EZW	embedded zerotree wavelet
FDOA	frequency-difference-of-arrival
GLR	generalized likelihood ratio
LPE	lowpass equivalent
LPI	low-probability of intercept
ML	maximum likelihood
RF	radio frequency
SNR	signal-to-noise ratio
SVD	singular value decomposition
TDOA	time-difference-of-arrival